Fermi National Accelerator Laboratory

FERMILAB-Conf-94/323-E

DØ

DØ Quantum Chromodynamics: A Compilation of Results Presented at DPF 1994

The DØ Collaboration

Fermi National Accelerator Laboratory
P.O. Box 500, Batavia, Illinois 60510

September 1994

Presented at the *Eighth Meeting of the Division of Particles and Fields of the American Phyiscal Society (DPF '94)*, Albuquerque, New Mexico, August 1-8, 1994

Operated by Universities Research Association Inc. under Contract No. DE-AC02-76CHO3000 with the United States Department of Energy

Disclaimer

TABLE OF CONTENTS

DØ Quantum Chromodynamics
A Compilation of Results Presented at DPF 1994

FERMILAB-Conf-94/323-E

Fermi National Accelerator Laboratory

Direct Photon Production at DØ

Salvatore T. Fahey

Michigan State University,
East Lansing, Michigan 48824-1116

Operated by Universities Research Association Inc. under Contract No. DE-AC02-76CHO3000 with the United States Department of Energy

DIRECT PHOTON PRODUCTION AT DØ

SALVATORE T FAHEY*
Physics-Astronomy Department, Michigan State University,
East Lansing, MI 48824-1116, USA

ABSTRACT

A preliminary cross section for the inclusive production of central isolated direct photons is presented, as measured by the DØ detector at the Fermilab Tevatron $p\bar{p}$ Collider. Photon candidates with transverse momentum greater than 9 GeV/c and within the pseudorapidity range $|\eta| < 0.9$ are considered. Selection criteria for photon candidates are discussed, as is the estimation of background contributions from jets. The cross section is found to be in good agreement with the next-to-leading-order (NLO) QCD prediction over the whole range of p_T.

1. Introduction

Direct photons have proved to be a valuable tool for studying QCD at hadron colliders.[1] Photons are a direct link to the parton level of the interaction, unlike jets which suffer from ambiguities in identification and energy measurement. At low E_T the dominant mode of production is from gluon-Compton scattering, which makes the outgoing photon a good probe of the incoming gluon. At Tevatron energies ($\sqrt{s} = 1.8$ TeV) the gluon distributions as low as $x_g = 0.001$ can be probed with the DØ detector.[2]

2. Trigger and Event Selection

DØ operates with a multi-tiered triggering system. The first level (called Level 0) consists of scintillator near the beam pipe which fires when a $p\bar{p}$ interaction is detected. The next level, Level 1, is a hardware trigger which makes fast sums of the electromagnetic energy in towers ($\eta = 0.2$, $\phi = 0.2$) in the calorimeter. There are three Level 1 triggers used in this analysis with thresholds of 2.5, 7, and 10 GeV. Level 2, a software based trigger, clusters the calorimeter cells and rejects the candidate if the longitudinal energy deposition is inconsistent with test beam electrons. The three Level 2 thresholds used are 6, 14, and 30 GeV.

Additional cuts are applied to the photon candidates off-line. An $|\eta| < 0.9$ cut is used to restrict candidates to the central region. The electromagnetic fraction of the calorimeter shower must be greater than 96% and the shower shape is required to be consistent with the shape of test beam electrons. An isolation cut of less than 2 GeV of E_T in the isolation cone ($0.2 < R < 0.4, R = \sqrt{\Delta\eta^2 + \Delta\phi^2}$) is applied. The missing E_T of the event is required to be less than 50% of the photon E_T (if the photon E_T is greater than 20 GeV) to reject electrons from W events.

*Representing the DØ Collaboration.

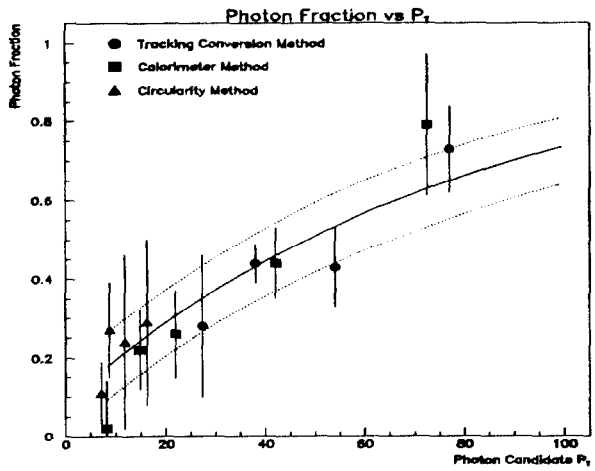

Fig. 1. Photon Fraction (γ) vs p_T^γ for the three methods of background subtraction. The solid line is a fit and the dotted lines are the errors of the fit.

3. Background Subtraction

The data sample detailed above contains a significant amount of background in the form of electromagnetic jets. These are mostly single isolated π^0's and η's which decay into two photons. At this p_T range the photons coalesce and mimic a single photon shower in the calorimeter. Fluctuations in the shower development make background subtraction on an event-by-event basis impossible. There are, however, methods by which the background can be subtracted on a statistical basis.

DØ uses three methods of background subtraction. They are all based on the relationship:

$$\gamma = \frac{\epsilon_\pi - \epsilon}{\epsilon_\pi - \epsilon_\gamma}. \tag{1}$$

where γ is the fraction of candidates that fulfill the selection criteria which are genuine direct photons, and ϵ_γ, ϵ_π, and ϵ are the fraction of candidates passing a specific cut for photons, background, and data respectively.

The first method uses the fact that the two-photon backgrounds tend to convert (produce e^+e^- pairs) roughly twice as often as single photons. This means that calorimeter showers from background develop earlier than single photon showers. The ratio of energy in the first layer of the calorimeter (EM1) to the total shower energy is used as a discriminant.

The second method is also based on backgrounds having a higher conversion probability. Conversions are tagged as tracks with twice minimum ionizing energy using the *dE/dx* measurement in the Central Drift Chambers.

The third method exploits the opening angle between the two photons from background sources. At lower p_T this angle is large enough to create an asymmetry in the

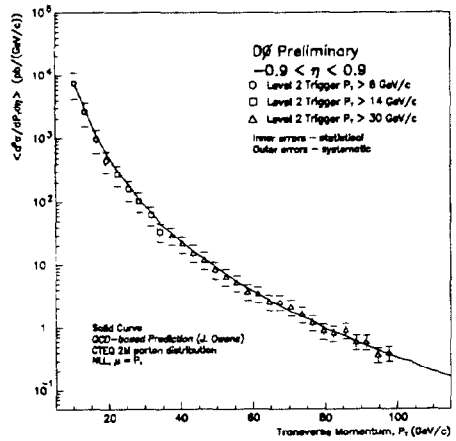

Fig. 2. Differential Direct Photon Cross Section vs. p_T.

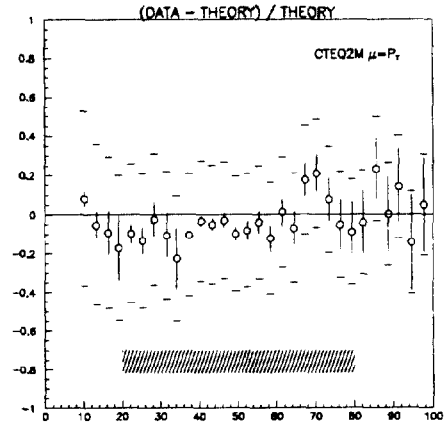

Fig. 3. Comparison between data and NLO QCD theory, CTEQ2M parton distributions.

calorimeter showers. The shower profile in the third layer of the calorimeter (at shower maximum) will look ellipsiodal for two photon showers and circular for single photon showers. The shower profile is diagonalized and a variable called circularity is defined as the ratio between the minor and major axis of the ellipse. For photons circularity should be close to unity, whereas for π^0's and η's this tends to smaller values. This method is only used up to 20 Gev, above which the opening angle between the two photons is too small.

A functional form of $\gamma(p_T)$ is obtained by fitting the three background subtraction methods and this function is used to subtract the background from the cross-section (see Fig. 1). The parameters in the fit are shifted by one standard deviation and the variation in $\gamma(p_T)$ is used as an estimate of the error.

4. Cross Section

The differential cross section vs. p_T is shown in Fig. 2. The theory prediction is generated from a Monte Carlo based on NLO QCD due to J. Owens with CTEQ2M parton distributions[3] and a renormalization scale of $\mu = p_T$. Figure 3 shows a plot of (data - theory) / theory to illustrate the good agreement between the two. The shaded band at the bottom of the plot corresponds to a $\pm 12\%$ normalization error due to luminosity uncertainty.

References

1. B. Bailey, J. F. Owens, and J. Ohnemus, *Phys. Rev.* **D46** (1992) 2018.
2. S. Abachi *et al.*, *Nucl. Instr. and Meth.* **A338** (1994) 185.
3. J. Botts *et al.*, *Phys. Lett.* **B304** (1993) 159.

Fermi National Accelerator Laboratory

Direct Photon Angular Distribution at DØ

Paul M. Rubinov

State University of New York at Stony Brook,
Stony Brook, New York 11794

Operated by Universities Research Association Inc. under Contract No. DE-AC02-76CHO3000 with the United States Department of Energy

DIRECT PHOTON ANGULAR DISTRIBUTION AT DØ

Paul M. Rubinov*
Physics Department, State University of New York at Stony Brook, Stony Brook, NY 11794, USA

ABSTRACT

A preliminary measurement of the $\cos\theta^*$ of direct photon events at $\sqrt{s} = 1.8$ TeV is presented, covering a range of $\cos\theta^*$ up to 0.9. The data are compared with next-to-leading-order predictions. We find good qualitative agreement with QCD predictions. We discuss the prospects of significantly reducing the systematic errors on this measurement.

1. Introduction

It has been pointed out by many authors that photons provide a good tool for studying QCD at hadron colliders [1,3]. In addition to the inclusive photon production cross section, photon angular distributions may also prove a valuable tool for testing QCD. At the energies considered for this analysis, the dominant QCD jet processes occur via an interchange of a gluon (spin 1) propagator. This produces the characteristic angular distribution $dN/d\cos\theta^* \propto (1-\cos\theta^*)^{-2}$, where θ^* represents the photon-jet center of mass (CM) polar angle between the beam and the outgoing photon. Photons, on the other hand, are produced predominantly through processes involving the exchange of a spin 1/2 quark, which produces a distribution $dN/d\cos\theta^* \propto (1-\cos\theta^*)^{-1}$ This means that at relatively large $\cos\theta^* \geq .8$, the increase in the rate of production relative to $\cos\theta^* = 0$ is much larger for jets than for photons. This makes sensitive tests of QCD possible, and the unparalleled angular coverage offered by the DØ detector at Fermilab promises to make it an important contributor to this field in the future.

However, the cross section for the production of jets is several orders of magnitude larger than that for photons, and can pose a significant background problem. The jets may fragment in such a way that a single neutral meson, such as a π^0 or an η, may carry most of the energy of the jet, and produce a signature in the detector which is very difficult to distinguish from that of a photon produced directly in the hard scattering.

2. Event Selection

The DØ detector and its triggering system have been described elsewhere.[2] For the preliminary analysis described here, it is sufficient to note that all candidate photons with a P_T in excess of 30 GeV/c were recorded. These candidates were selected by requiring standard DØ photon cuts (as described in ref 5.) In order to extract the angular distribution of the photons, the data were also restricted to the central region

*representing the DØ Collaboration.

of the detector where the acceptance for photons is understood and where methods of background subtraction are currently available. Furthermore, for this preliminary analysis, we choose to restrict the data to regions where the acceptance is flat so that no acceptance corrections are necessary.

In order to be able to reconstruct the kinematics of the event in the CM frame, it is also necessary to know the direction of the recoiling jets. Therefore we require that at least one jet, which passes all standard jet cuts, was found in the event, and that the total missing $E_T \leq 0.3 P_{t\gamma}$. Furthermore, in order to retain the simplicity of the $2 \rightarrow 2$ process, we take the vector sum of all jets which are in the opposite hemisphere from the photon in ϕ. The jets on the same side are ignored. The measured quantities we extract from each event are η_γ, $E_{T\gamma}$, and η_{jet}. From these, we can form the CM quantities and the boost of that system relative to the lab,

$$\eta^* = \frac{\eta_\gamma - \eta_{jet}}{2}, \qquad \eta_{boost} = \frac{\eta_\gamma + \eta_{jet}}{2}, \qquad P^* = P_T \cdot \cosh \eta^*, \qquad \cos\theta^* = \tanh \eta^* \quad (1)$$

Since we wish to cover as large a range in $\cos\theta^*$ (and therefore η^*) as possible, while requiring the photon to be central, we allow the recoil jet to cover a large range of pseudo-rapidity. And in order to avoid acceptance corrections, we divide the data into 3 regions, each of which covers a range of 0.8 in η^* and η_{boost}. These regions form squares in η^* and η_{boost} space. The regions and their relationship to the η_{boost} and η^* axis are shown in Fig 1. The final data sample is seen to lay within these regions. We also note that since we are interested only in $|\cos\theta^*|$, data appears on both sides of the η^* axis. Furthermore, we must require that all events in a particular region are above a certain P^*, which is dictated by $P^*_{min} = Pt_{min} \cdot \cosh \eta^*_{max}$, so that all events are assured to be above the trigger threshold.

In order to extract only the $\cos\theta^*$ dependence, we normalize between regions in the areas where they overlap. Furthermore, we normalize the curve to one in the first three bins. This allows us to compare the shape of the distribution with the Next to Leading Log (NLL) theoretical prediction.[1] When projecting onto the $\cos\theta^*$ axis, we always take only the data from the lower region. Thus for bins of size 0.1 in $\cos\theta^*$, the data for the first six bins ($0 \leq \cos\theta^* < 0.6$) comes from the region closest to the origin in Fig 1, the next two bins (($0.6 \leq \cos\theta^* < 0.8$) from the middle region, and the last bin, covering $0.8 \leq \cos\theta^* \leq 0.9$, is from the outermost region.

3. Background Subtraction

In order to subtract the background due to jets in this sample, we apply the calorimeter method,[5] which has been described previously, to the data in region 1 only ($\cos\theta^* \leq 0.6$). This results in a photon purity of ~ 0.52 . We are, at this time, unable to do the background subtraction for regions 2 or 3. Therefore we assume that the background in these regions is due to jets and has the same angular distribution as the jets sample. We select the data sample for estimating the angular distribution of the background by taking the inclusive jet sample above 30 GeV and randomly assigning one jet the role of the photon. These events are then required to pass all cuts applied to the photon sample. Knowing the angular distribution of the background and the relative normalization of signal and background allows us to extract the signal as

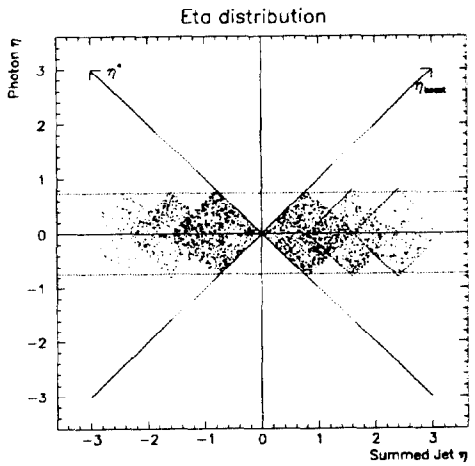

Fig. 1. Plot of candidates in η_γ vs η_{jet} for the three regions. The lines at 45° are the η_{boost} and η^* axis.

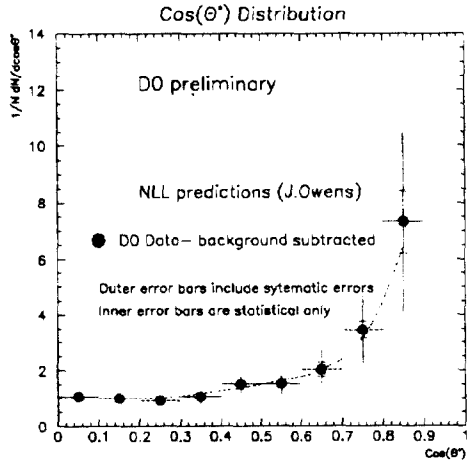

Fig. 2. Plot of the normalized $\cos\theta^*$ distribution compared to normalized NLL prediction.

a function of $\cos\theta^*$. The final normalized and background-subtracted data sample is shown in Fig 2. Also shown is the NLL Monte Carlo prediction.

4. Conclusions

We find that the NLL theory is in excellent qualitative agreement with our background-subtracted data in the range of $\cos\theta^* \leq 0.9$, which extends the range of previously published measurements of $\cos\theta^*$ of photons at the Tevatron.[4] We note that our errors are dominated by the need to extrapolate the background subtraction from $\cos\theta^* = 0.6$ to $\cos\theta^* = 0.9$. Additional studies of the calorimeter method for estimating the background should enable us to measure the background as a function of $\cos\theta^*$ over the full range from 0 to 0.9, and thus significantly reduce the systematic errors in the last three bins of Fig 2. The higher statistics data sample from the 1994-95 Tevatron run will also reduce the error associated with the matching of the three different regions, and allow us to move from qualitative agreement to precision quantitative tests of QCD.

References

1. B. Bailey, J. F. Owens, and J. Ohnemus, *Phys. Rev.* **D46**(1992) 2018.
2. S. Abachi, et al., *Nucl. Instr. and Meth.* **A338**(1994) 185.
3. Gregory R. Snow, et al., Published in *DPF Conference Proceedings* (1992) 971.
4. F. Abe, et al., *Phys. Rev. Lett.* **71** (1993) 679.
5. S. Fahey, "Direct Photon Production at DØ " in the these proceedings.

Fermi National Accelerator Laboratory

Inclusive Jet Cross Sections at the DØ Detector

Victor Daniel Elvira

Fermi National Accelerator Laboratory,
P.O. Box 500, Batavia, Illinois 60510

Operated by Universities Research Association Inc. under Contract No. DE-AC02-76CHO3000 with the United States Department of Energy

INCLUSIVE JET CROSS SECTIONS AT THE DØ DETECTOR

VICTOR DANIEL ELVIRA*
Physics Dept., Fermilab–Universidad de Buenos Aires
P.O.Box 500, Batavia, Illinois 60510, U.S.A.

ABSTRACT

The DØ calorimeter has uniform response and hermetic coverage for detection of jets produced in $p\bar{p}$ collisions out to a pseudo–rapidity $|\eta| = 4.1$. Based on a 13 pb^{-1} data sample recorded during the $1992 - 1993$ run, we present a measurement of the inclusive differential jet cross section as a function of the jet transverse energy for $|\eta| \leq 3$. The experimental results are compared to the next–to–leading order (NLO) theoretical predictions currently available.

1. Introduction

The availability of a QCD theoretical prediction in the next–to-leading order approximation,[1,2] has increased the interest in the measurement of the inclusive jet cross sections. The inclusive differential jet cross section is defined as:

$$\frac{d^2\sigma}{dE_T d\eta}(\bar{p}p \rightarrow jet + X)$$

and has been measured accurately by the CDF collaboration[3] in the central pseudo–rapidity region ($0.1 < |\eta| < 0.7$). There is also a measurement by the UA2 collaboration[4] in the pseudo–rapidity range $|\eta| < 2$. Using its excellent calorimetry and rapidity coverage, DØ has extended the measurement to previously unexplored rapidity regions ($|\eta| < 3$) allowing a more complete test of the QCD predictions.

2. DØ Calorimetry

The DØ calorimetry[5] consists of three liquid argon calorimeters divided into several electromagnetic, fine hadronic and coarse hadronic modules. The calorimeters are $7 - 9$ interaction lengths deep and provide uniform and hermetic coverage out to $|\eta| = 4.1$. The energy and position resolution for particles passing the calorimeters is excellent, due to the fine transverse segmentation, 0.1×0.1 in $\eta - \varphi$ space. The energy response is linear within 0.5% and the e/π response ratio is $1.02 - 1.09$. The energy resolutions for electrons and pions are $15\%/\sqrt{E}$ and $50\%/\sqrt{E}$ respectively.

*Representing the D0 Collaboration.

3. Data Selection and Reconstruction

Jets are reconstructed with a fixed cone algorithm (cone size $R = 0.7$) in this analysis. Every 0.1×0.1 tower with more than 1 GeV is used as a seed to find a jet. All the neighbor towers with $E_T > 1$ GeV are joined to the seeds and a cone of $R = 0.7$ is drawn around the center (η_o, φ_o) of the energy cluster. The E_T of the jet is calculated as the sum of the E_{T_i}'s deposited in each tower inside the cone and the position (η_o,φ_o) is obtained from the x, y, and z components of the energy in each tower:

$$E_x = \sum_i E_{x_i} \qquad E_y = \sum_i E_{y_i} \qquad E_z = \sum_i E_{z_i}$$
$$tan\,\varphi_o = \frac{E_y}{E_x} \qquad cos\,\theta_o = \frac{E_z}{\sqrt{E_x^2+E_y^2+E_z^2}} \qquad \eta_o = -ln\left(tan\,\frac{\theta_o}{2}\right)$$
$$E_T = \sum_i \sqrt{E_{x_i}^2 + E_{y_i}^2}$$

A new cone is drawn around the new center, the jet variables are recalculated and the process is repeated until the centroid (η_o, φ_o) becomes stable. If two jets share more than 50% of the E_T of the smaller one, they are merged. In addition, the minimum possible E_T for a jet is 8 GeV. Jet finding efficiency is $> 99\%$ above 20 GeV in all η regions.

Three different trigger levels are involved in the online selection of jet events. The level Ø (LØ) consists of a set of scintillator counters which fire the trigger when a non-diffractive interaction takes place. Level 1 (L1) is a hardware trigger which does a fast sum of the transverse energy deposited in a 0.2×0.2 trigger tower. The event passes the L1 trigger if there is a minimum amount of E_T in a specified number of trigger towers. The level 2 (L2) is a software trigger which runs a fast version of the fixed cone algorithm and sets a condition on the jet E_T. In the inclusive jet analysis, five different thresholds were used at L2: 20, 30, 50, 85 and 115 GeV. In all the cases except the highest E_T threshold and sometimes the second highest one, a cut on the z coordinate of the interaction vertex ($|z| < 10.5$ cm) was applied to take advantage of the calorimeters pseudo-projective geometry. In addition, low E_T triggers are heavily prescaled to lower the event rates and avoid bandwidth saturation. The trigger information was used in the E_T, η ranges where they are more than 95% efficient.

Several offline cuts were applied to remove noise and background. The standard jet cuts are defined as follows:

$$\begin{aligned} &\text{EMF} \in [0.05, 0.95] \\ &\text{HCF} > 0.1 \\ &\text{CHF} < 0.4 \quad , \end{aligned}$$

where EMF and CHF are the fractions of transverse energy deposited in the electromagnetic and the coarse hadronic modules of the calorimeters. HCF is the ratio E_T of the second most energetic cell to the most energetic cell. An additional cut, based on the missing transverse energy of each event, is applied to remove electronic noise and cosmic showers at high E_T. The cut is defined as:

$$\frac{\not{E}_T}{E_T^{leading\,jet}} < 0.7 \quad ,$$

where $\not\!\!E_T$ is the event missing E_T and the leading jet is the one with the highest E_T. The overall efficiency for these cuts is greater than 90% in all pseudo–rapidity regions. The noise rejection is greater than 98%. The data used in this analysis were taken during the 1992 – 1993 run period and correspond to a total luminosity of 13 pb^{-1}.

4. Jet Energy Scale and Resolution Effects

A fraction of the jet energy that enters the calorimeters is lost in uninstrumented areas or leaked outside the cone by showers of particles produced inside the calorimeters. In addition, there is some spurious energy within the jet cone limits coming from the underlying event and uranium radiation. The jet E_T must be corrected back to the parton jet level[1,2] to allow comparison with theoretical predictions. The missing E_T projection fraction method (MPF)[6] was used in a $\gamma - jet$ event sample to obtain the jet calibration with respect to the electromagnetic scale in the central calorimeters. The calibration was extended to the forward η region using energy balance in the transverse plane on a sample of dijet events. The electromagnetic scale was calibrated using LEP results on Z mass and DØ measurements on $Z \rightarrow e^+e^-$. Finally, the underlying event and uranium noise contamination was subtracted.

The fractional jet E_T resolution as a function of E_T is approximately $85\%/\sqrt{E_T}$ and was also determined from collider dijet and $\gamma - jet$ data for each η region in which the jet cross section was measured. The jet E_T spectrum in a particular η region was corrected for resolution smearing by assuming a hypothetical unsmeared cross section which is a function of E_T and η. This function was smeared with the measured E_T resolution and fit to the data. Finally, the data was corrected by the ratio of the hypothetical cross section to the smeared hypothetical cross section.

The η resolution was studied with a Monte Carlo simulation. Within the E_T and η range the cross sections were measured, the η resolution is less than 0.04. No correction was applied to the jet cross sections since the η resolution effect on the jet E_T spectrum is less than 1% in the central region and up to a 2.5% in the forward regions.

5. Inclusive Differential Jet Cross Sections

The inclusive jet cross sections measured with the DØ detector in different pseudo–rapidity regions are shown in Fig. 1. In the most central η bin, $|\eta| < 0.5$, the statistical errors are less than 5% below 300 GeV. The systematic uncertainty due to the energy scale correction and unsmearing procedure is $\approx 35\%$. Other uncertainties from acceptance corrections and contamination contribute a $\approx 7\%$. The error in the luminosity calculation is 12%.

The measurements are compared to EKS[1,2] theoretical predictions in the (NLO) approximation using CTEQ2M parton distribution functions.[7] There is good qualitative agreement between theory and experiment over the whole pseudo–rapidity range that was measured. The predictions are also included within the limits of the total systematic errors associated with the measurement in all the η regions.

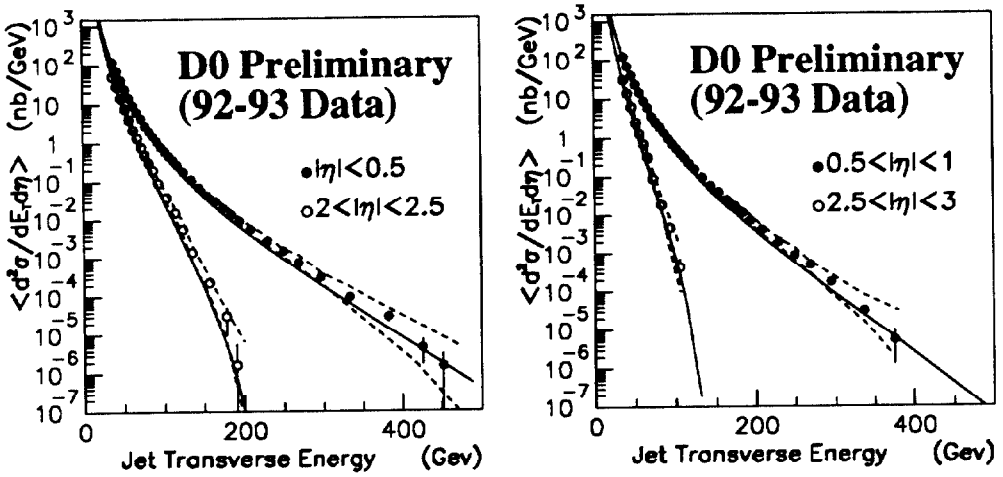

Fig. 1. Inclusive jet cross sections measured with the DØ detector in four different η regions. The bars are statistical errors and the band is the uncertainty from the energy scale correction. The EKS (NLO) predictions using CTEQ2M parton distribution functions are shown in solid lines.

References

1. S.D.Ellis, Z.Kunszt, D.Soper, *Phys. Rev.* **D40** (1989) 2188.
2. S.D.Ellis, Z.Kunszt, D.Soper, *Phys. Rev.* **D64** (1990) 2121.
3. F.Abe et al., *Phys. Lett.* **B68** (1992) 1104.
4. J.Alitti et al., *Phys. Lett.* **B257** (1991) 232.
5. The DØ Collaboration, *Nucl. Instr. and Methods* **A338** (1994) 185.
6. DØ Collaboration, H.Weerts, "Proceedings of the 9^{th} Topical Workshop in $p\bar{p}$ Collider Physics", Tsukuba (1993), edited by K.Kondo.
7. James Botts et al., *Phys. Lett.* **B304** (1993) 159.

Fermi National Accelerator Laboratory

A Study of the Inclusive Jet Cross Section as a Function of Jet Cone Size with the DØ Detector

Mrinmoy Bhattacharjee

University of Delhi,
Delhi 110007, India

Operated by Universities Research Association Inc. under Contract No. DE-AC02-76CHO3000 with the United States Department of Energy

A STUDY OF THE INCLUSIVE JET CROSS-SECTION AS A FUNCTION OF JET CONE SIZE WITH THE DØ DETECTOR

MRINMOY BHATTACHARJEE*
Dept. of Physics & Astrophysics, University of Delhi, Delhi 110007,INDIA

ABSTRACT

Based on a $13pb^{-1}$ data sample recorded at DØ during the 1992-1993 run, we present preleminary results on the cone size dependence of the inclusive differential jet cross-section. The study has been done with three cones sizes, 0.7, 0.5 and 0.3. Cross-sections have been corrected for trigger efficiencies and standard jet cut efficiencies. We also present comparisons to next-to-leading order QCD calculations.

1. Introduction

Leading order, $O(\alpha_s^2)$, QCD describes fairly well the inclusive jet cross-section, $\sigma(p\bar{p}) \rightarrow jet + X$, in central pseudo-rapidities, $|\eta| < 1$, and over a wide range of centre of mass energies, $0.063TeV < \sqrt{s} < 1.8TeV$ [1], [2], [3]. However, leading order comparisions include a $30 - 50\%$ theoretical normalization uncertainity. Recent next-to-leading order, $O(\alpha_s^3)$, calculations reduce the theoretical uncertainities to $\sim 5\%$ [4], [5].

At NLO, QCD predicts the inclusive jet cross-section to be a function of the jet cone size($R=\sqrt{(\delta\eta)^2 + (\delta\phi)^2}$). Also, it predicts that the cross-section goes down with cone size. These can be tested with data.

The present study is done on a $13pb^{-1}$ data sample taken during the 1992-1993 data run at the Fermilab Tevatron Collider. A study of the cone size dependence of the inclusive jet cross-section has been done, using three different cone sizes, R=0.3,0.5 and 0.7. The η dependence of the inclusive jet cross-section for all the cone sizes are given over (a) $-1 < \eta < 1$, (b) $2 < |\eta| < 3$ and $30GeV \leq E_T \leq 480GeV$.

2. Data Sample and Analysis

The DØ detector described elsewhere [6], has a uranium-liquid argon calorimeter with a full coverage for a pseudo-rapidity range of $|\eta| < 4.1$, for detection of final state jets. The calorimeters are azimuthally symmetric and have electromagnetic and hadronic resolutions of $15\%/\sqrt{E}$ and $50\%/\sqrt{E}$, respectively.

The detector is read out if a hardware jet trigger based on E_T in calorimeter towars, followed by a software jet trigger, is satisfied. The integrated luminosity is $13pb^{-1}$ with a luminosity uncertainity of 12%.

*Representing the D0 Collaboration.

The jets were then reconstructed with cone algorithms with radii of 0.3, 0.5 and 0.7. The E_T of the jet is defined as the sum of E_T of each tower within the cone. After forming all the jets, jets sharing more than 50% of their energies were merged. The reconstruction efficiency is $> 99\%$ above 25GeV and for all η [7].

Backgrounds arising from isolated noisy electronic cells were eliminated by using two cuts. The first requirement is, the fraction of energy deposited in the electromagnetic(EM) modules must be within 5 and 95%. Secondly, the ratio between the second most energetic cell and the most energetic cell in a jet is required to be greater than 10%. Main Ring jets were eliminated by requiring the fraction of energy deposited in the coarse hadronic(CH) modules to be less than 40%. Backgrounds from cosmic ray bremsstrahlung were eliminated by requiring the missing E_T in an event to be less than 70%. Efficiencies of these cuts are more then 90% for all η's and for all three cone sizes(0.3,0.5,0.7) [8].

The E_T of jets have been corrected to account for nonlinearity of the calorimeter. These energy scale corrections are around 30% for $30GeV \leq E_T \leq 450GeV$ in the central region. This is the biggest source of systematic error and it becomes worse in the forward region as the cross-section falls more steeply in the forward region than in the central region. We have not yet attempted to unsmear the effects of detector E_T and η resolution. As described elsewhwere in these proceedings[9], the E_T resolution distorts the steeply falling cross-section but effect of the η resolution is negligible.

3. Results and Discussion

Fig.1 shows the ratio of cross-section for jet cone size 0.5 to that of jet cone size 0.7 and the same for jet cone size 0.3, in the central region($-1 < \eta < 1$). By taking the ratio, we have eliminated luminosity uncertainties and error from energy scale correction have been minimized. We have also made comparisions with NLO theory prediction using CTEQ2M parton distribution function. We have used two renormalization scales, $\mu = E_T$ and $E_T/4$. The theory is Jetrad which is a NLO loop level jet Monte Carlo(W.Giele et al.). However, the data has not been unsmeared. The error band that runs along the data points in Figs.2 and 3, is our estimate of systematic errors that will arise from unsmearing of the data. This systematic error is around 10% for jet cone size 0.5 and is double for jet cone size 0.3. While the ratio shows some dependence on E_T, it is not inconsistent with being flat, as predicted by NLO-QCD for both $R = 0.5/0.7$ and $R = 0.3/0.7$, given our systematic errors. As expected the inclusive jet cross-section goes down with jet cone size(R). We also observe sensitivity to the choice of the renormalization scale, μ. In future, we will extend these comparions to the forward region ($2 < |\eta| < 3$). Also, to quantify these results we need a better understanding of our systematics.

References

1. T. Akesson et al.(AFS Collaboration), *Phys. Lett.* **B 123** (1983) 133.
2. J.Alitti et al.(UA2 Collaboration), *Phys. Lett.* **B 257** (1991) 232.
3. F.Abe et al.(CDF Collaboration), *Phys. Rev. Lett.* **61** (1988) 613.
4. F.Abe et al.(CDF Collaboration), *Phys. Rev. Lett.* **68** (1992) 1104.
5. S.Ellis et al. *Phys. Rev. Lett.* **64** (1990) 2121.
6. The DØ Collaboration, *Nucl. Instr. and Methods* **A338** (1994) 185.

7. A.Milder, Ph.D Thesis, University of Arizona (1993)
8. M.Bhattacharjee et al., "Efficiencies of the Standard Jet Cuts for Cone Sizes:0.3,0.5,0.7.", DØ internal note DØ 2197 (1994).
9. V.D.Elvira, "Inclusive Jet Cross Section at the DØ Detector." in the same proceedings.

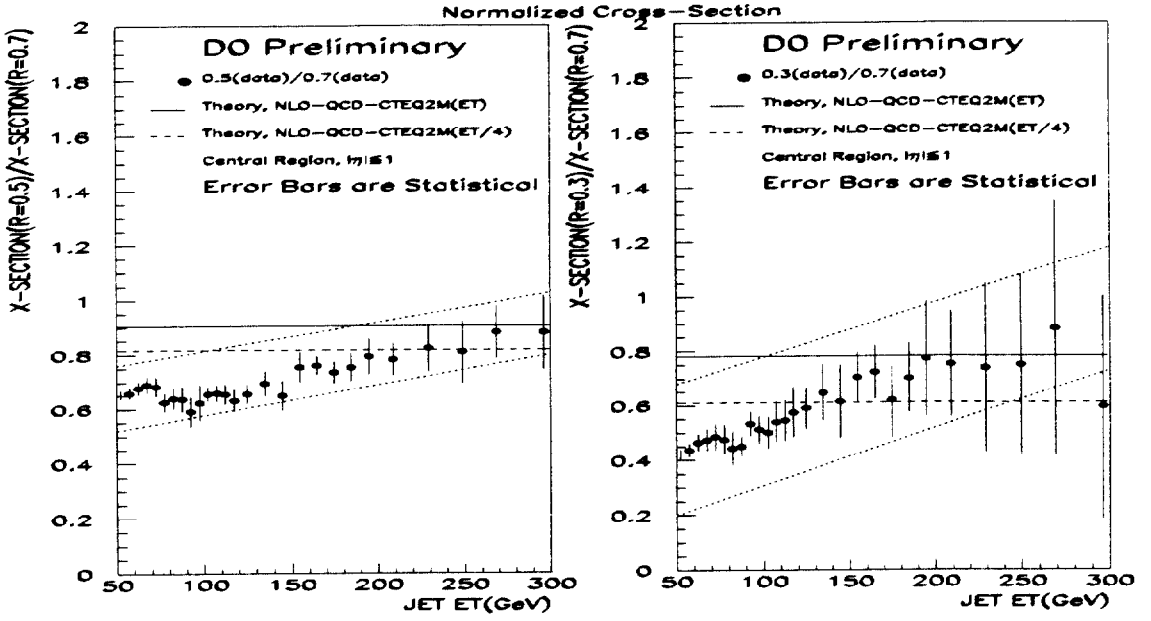

Fig. 1. Ratio of data cross sections, 0.5/0.7 (data) and 0.3/0.7, respectively, as compared to theory(Jetrad).

Fermi National Accelerator Laboratory

Measurement of the Triple Differential Inclusive Dijet Cross Section, $d^3\sigma/dE_T d\eta_1 d\eta_2$ in $p\bar{p}$ Collisions at $\sqrt{s}$ = 1.8 TeV

Freedy Nang

Brown University,
Providence, Rhode Island 02912

Operated by Universities Research Association Inc. under Contract No. DE-AC02-76CHO3000 with the United States Department of Energy

MEASUREMENT OF THE TRIPLE DIFFERENTIAL INCLUSIVE DIJET CROSS SECTION, $d^3\sigma/d\mathrm{E_T}d\eta_1 d\eta_2$ IN $P\bar{P}$ COLLISIONS AT $\sqrt{s} = 1.8$ TEV

FREEDY NANG*
Department of Physics, Brown University, Providence, RI 02912

ABSTRACT

Experimental results from a measurement of the inclusive differential dijet cross section, $d^3\sigma/dE_T d\eta_1 d\eta_2$ are presented. These events were produced in the Fermilab Tevatron $p\bar{p}$ collider at a center of mass energy of $\sqrt{s} = 1.8$ TeV and collected with the DØ detector. The data consists of approximately 13 pb^{-1} taken during the 1992-1993 run. Comparisons to Next-to-Leading Order perturbative QCD predictions are made.

1. Introduction

The gluon contribution for the parton distribution functions (PDF) is not well known. The inclusive differential dijet cross section, $d^3\sigma/dE_T d\eta_1 d\eta_2$, can provide information about both quark and gluon distribution functions. Additionally, the excellent η coverage of DØ allows us to probe the extreme values of $x \sim 0.002$ and $x > 0.8$.

2. Event Selection Criteria

The DØ detector has been described elsewhere.[1] The trigger consists of two levels. The hardware triggers require one to four towers (0.2×0.2 in $\eta - \phi$ space) above some E_T threshold. The software triggers require a jet of cone size 0.7 at different thresholds mapping the E_T spectrum. Offline, we apply standard quality cuts[2] to ensure good jets, and require at least two jets in the event, where jets are ordered in decreasing E_T.

3. Preliminary Results

For this analysis, we symmetrize the cross sections: we look at the two leading jets letting the leading jet to be jet 1 and the second leading jet to be jet 2 and vice versa. Figure 1 shows the cross section $\langle d^3\sigma/dE_T d\eta_1 d\eta_2\rangle_{E_T}$, integrated over the range $55 \leq E_T^{J1} \leq 65$ GeV, as a function of η_1 and η_2. The detector acceptance goes out to $|\eta| \leq 4.1$ and the cutoff of the cross section is solely due to kinematics. We choose to plot the cross section in two different ways:

*Presented for the DØ Collaboration

(1)$\langle d\sigma/dE_T^{J1}\rangle_{\eta_1,\eta_2}$ vs. E_T^{J1}; where we plot the E_T of jet 1 for different η values of jet 2 while requiring jet 1 to be central.

(2) $\langle d\sigma/d\eta_2 \times sign(\eta_1)\rangle_{E_T,\eta_1}$ vs. $\eta_2 \times sign(\eta_1)$; the more extreme x values are accessible when both outgoing partons are on the same side of the detector (in η). The variable $\eta_2 \times sign(\eta_1)$ plots the case where both jets are on the same side of the detector on the positive x-axis and jets on the opposite sides of the detector on the negative x-axis. This method of plotting the cross section accentuates the effect of the very small and very large x PDF's.

Figures 2 and 3 show the data compared to NLO theoretical calculations using the JETRAD parton level event generator.[3] The error bars indicate the statistical error and the dotted lines indicate the systematic error due to the jet energy scale. The calculations have been smeared with a parametrization of our jet resolution. Figure 2 shows good agreement with NLO. Giele *et al.*[3] have shown that the NLO cross section rises compared to LO as one moves forward in the η of jet 2 thereby indicating that the data favors NLO. Figure 3 shows the cross section, $\langle d\sigma/d\eta_2 \times sign(\eta_1)\rangle_{E_T,\eta_1}$, as a function of $\eta_2 \times sign(\eta_1)$ for $45 \leq E_T^{J1} < 55$ GeV and $2.0 \leq |\eta_1| < 3.0$. Again, the data is in good agreement with the NLO theoretical predictions.

Figure 4 shows that the shape of the cross section is insensitive to the renormalization scale for the theory for $|\eta| < 3$. Similarly, figure 5 shows the insensitivity of the data to the energy scale for the same η region.

In Figure 6, a comparison is made between the theoretical predictions for $\langle d\sigma/d\eta_2 \times sign(\eta_1)\rangle_{\eta_1,\eta_2}$, using various parton distribution functions. Each of the theoretical predictions for the cross section for $45 \leq E_T^{J1} < 55$ GeV and $2.0 \leq |\eta_1| < 3.0$, using the GRV,[4] MRSD-[5] and CTEQ2ML.[6] Each one is normalized to the theoretical prediction using CTEQ2M.

4. Conclusions and Future Plans

We have presented preliminary measurements of the inclusive triple differential dijet cross section, $d^3\sigma/dE_T d\eta_1 d\eta_2$. Comparisons of the preliminary measurements with NLO pQCD theoretical predictions show that our data agrees with the NLO predictions. In the future, we hope to use the DØ measurements to compare and differentiate between various parton distribution functions.

References

1. S. Abachi *et al.*, (DØ Collaboration), *The DZero Detector*, NIM **A338**:185 (1994).
2. See V. D. Elvira's talk in these Proceedings.
3. W.T. Giele, E.W.N. Glover, D.A. Kosower, *The Two-Jet Differential Cross Section at $O(\alpha_s^3)$ in Hadron Collisions*, Fermilab Preprint FERMILAB-Pub-94/070-T (1994).
4. M. Gluck, E. Reya, A. Vogt, Z. Phys. **C53**, 127 (1993).
5. A.D. Martin, W.J. Stirling, R.G. Roberts, Phys. Lett. **B306**, 145 (1993); Erratum-*ibid.***B309**, 492 (1993).
6. J. Botts, *et al.*, (CTEQ Collaboration), , *CTEQ Parton Distributions and Flavor Dependence of Sea Quarks*, Phys. Lett. **B304**: 159-166, (1993).

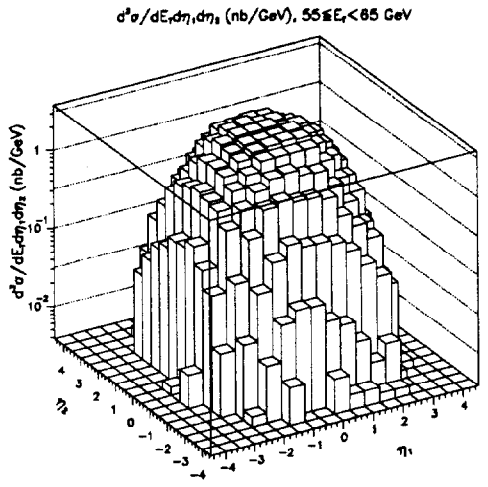

Fig. 1. $\langle d^3\sigma/dE_T d\eta_1 d\eta_2 \rangle_{E_T}$ for $55 \leq E_T^{J1} < 65$ GeV

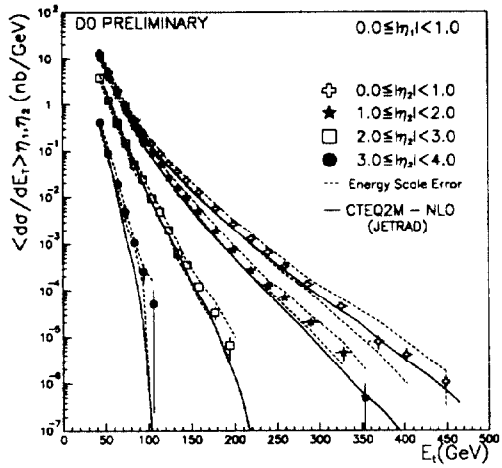

Fig. 2. $\langle d\sigma/dE_T^{J1} \rangle_{\eta_1,\eta_2}$ for $0. \leq |\eta_1| < 1.0$

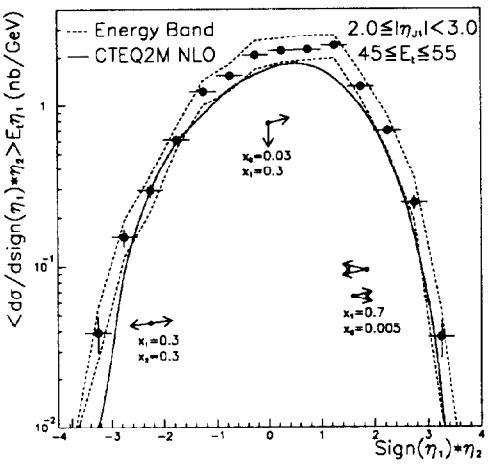

Fig. 3. $\langle d\sigma/d\eta_2 \times sign(\eta_1) \rangle_{E_T,\eta_1}$ for $45 \leq E_T^{J1} < 55$ GeV and $2.0 \leq |\eta_1| < 3.0$

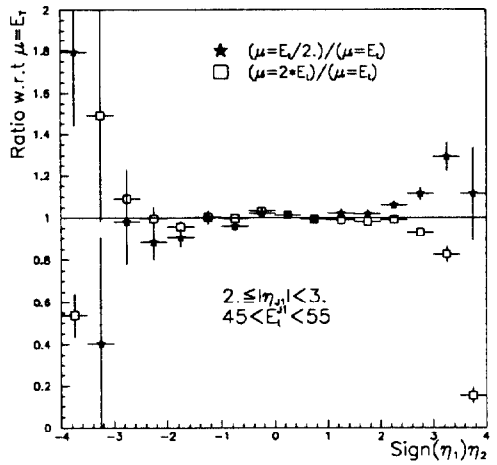

Fig. 4. Systematic Study of the Renormalization Scale

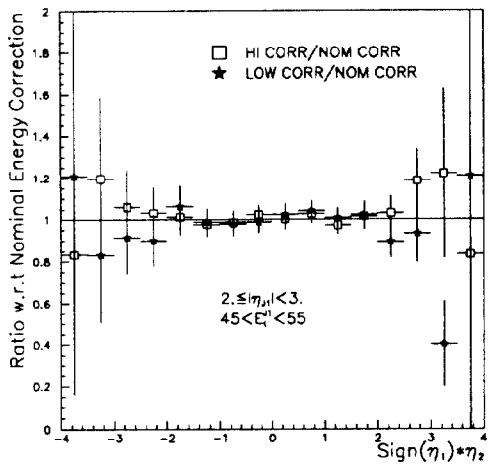

Fig. 5. Systematic Study of Energy Scale Correction

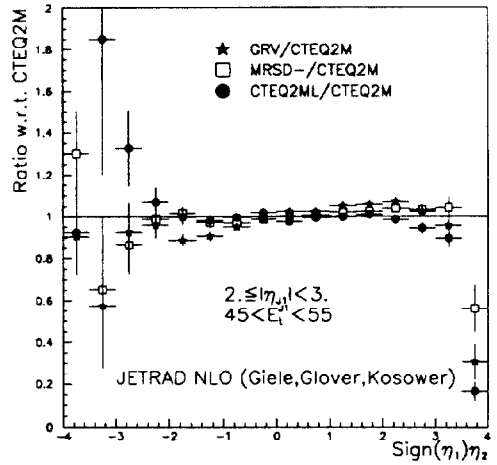

Fig. 6. Comparison of the theoretical prediction using different PDF's

Fermi National Accelerator Laboratory

Measurement of Jet Shapes in $p\bar{p}$ Collisions at DØ

Brad Abbott

Purdue University,
1396 Physics Building, West Lafayette, Indiana 47907-1396

Operated by Universities Research Association Inc. under Contract No. DE-AC02-76CHO3000 with the United States Department of Energy

MEASUREMENT OF JET SHAPES IN $P\bar{P}$ COLLISIONS AT D0

BRAD ABBOTT*
Department of Physics, Purdue University, 1396 Physics Building, West Lafayette, IN 47907-1396, USA

ABSTRACT

The distribution of the transverse energy flow in a jet has been measured in $p\bar{p}$ collisions at $\sqrt{s} = 1.8$ TeV at the Fermilab collider using the DØ detector. These measurements of jet shape are made at the central region of pseudo-rapidity and in different regions of jet transverse energy. Comparisons are made with next-to-leading-order QCD.

1. Introduction

Recent advances in the theoretical understanding of jet production at hadron colliders permit quantitative comparisons to experiment.[1] Next-to-Leading order (NLO) predictions at α_s^3 are possible for many hard QCD processes. These predictions determine the transverse energy deposition in a jet. One difficulty with jet physics is the definition of a jet. At the basic theoretical level, a jet is composed entirely of partons, i.e. quarks and gluons, and no fragmentation effects are included. At leading order (LO) only two final state partons are present, and the jet shape is simply a delta function at the parton's coordinates. At NLO, jet shapes becomes more complicated because there can be three final state partons. Depending on final state clustering algorithms, one or two partons may reside in a final state jet. The DØ detector[2] is ideal for measuring the shape of a jet due to the calorimeter's fine segmentation and high eta coverage. Other experiments have measured the transverse energy flow[3,4] with tracking chambers, considering only the energy carried by charged particles. In the measurement using the DØ calorimeter, both neutral and charged particles contribute to the jet shape.

2. Experimental Measurement of Jet Shape

Jets are found using the fixed cone algorithm with radius $R = \sqrt{\Delta\eta^2 + \Delta\phi^2} = 1.0$. A large radius was used in order to minimize out-of-cone effects. To study the internal structure of jets by measuring the transverse energy flow, the jet cone is divided into 10 subcones around the jet axis with equal thickness ($= 0.1$ in $\eta - \phi$ space). The integrated transverse energy in a subcone is measured as a function of the radius, r, of the subcone:

$$\rho(r) = \frac{\sum_{x=0}^{r} E_T(x)}{\sum_{x=0}^{R} E_T(x)}$$

*Representing the DØ Collaboration.

3. Data Sample and Cuts

Cuts were designed to remove trigger biases and to remove bad jets caused by hot cells and main ring contamination. The E_T of the leading jet that was reconstructed with a cone size of 0.7 was required to be in the 95% efficiency range for the trigger bit which fired. The vertex was required to be within $\pm$ 30 cm to keep the towers projective. Each jet in the event was required to pass the DØ standard good jet cuts.

4. Corrections to the Data

The jet energy distribution must be corrected for energy from the underlying event, zero suppression and for the jet energy scale. The underlying event and zero suppression artificially increase the energy in a jet. The jet energy scale correction boosts the energy of a jet between 20% and 25%. The magnitude of the underlying event and zero suppression effects were measured from a minimum bias run. The underlying event was constant in E_T at 0.55$\pm$ 0.1 GeV/$\eta \cdot \phi$. The zero suppression increase was constant in energy at 1.36$\pm$ 0.2 GeV/$\eta \cdot \phi$. Both of these effects were subtracted from each individual subcone.

5. Effects of the Calorimeter

Some effects of the calorimeter must be removed before comparing to partonic theory. The calorimeter affects the jet shape in two ways: a non-linear response narrows the jet shape and showering widens the jet shape. Monte Carlo simulations were used to determine the effects of the calorimeter on the jet shape. Because the effects of the calorimeter depend on the fragmentation of the jet, three different Monte Carlo simulations were used. The jet shape was determined before calorimeter effects by measuring the energy flow using only the fragmented particles. The jet shape after calorimeter showering was found by using a detector simulator (GEANT)[5] and measuring the energy flow using the calorimeter cells. The difference between the two measurements gives the calorimeter correction factors.

6. Systematic Errors

The systematic errors from underlying event, zero suppression and the jet energy scale on the jet shape were found by varying each correction within errors. The error on the calorimeter correction factors were assigned to accommodate the extreme values among the different Monte Carlo used to the find the corrections factors. An error of approximately 1% was assigned for biases due to triggers and the DØ standard good jet cuts. These five errors were added in quadrature to the statistical errors to get the final total error on the jet shape. The largest errors, approximately 2%, are due to the correction factors and to the uncertainty in the jet energy scale. The jet energy scale error is related to binning, allowing jets that were in previous bins to populate the region of interest. The errors due to the uncertainty in the underlying event and zero suppression are small, on the order of 0.5%.

7. Theory

The data can be compared to JETRAD,[1] a computer generated exact NLO tree and loop level theoretical prediction. The theoretical jet shape was determined for

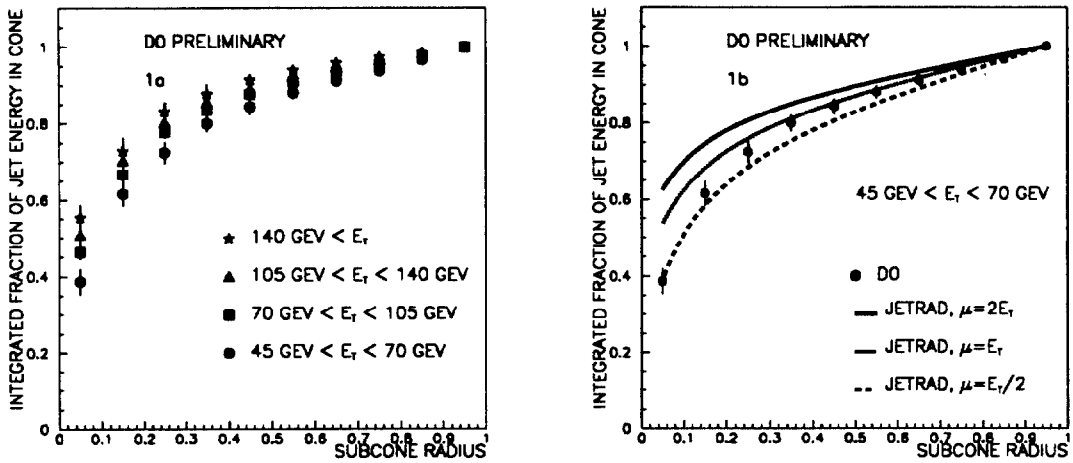

Fig. 1. (a) The jet shape for four different E_T regions. (b) NLO partonic theory vs Data.

three different renormalization scales, $\mu = 2E_T$, E_T, and $E_T/2$. There are many different structure functions currently available and the CTEQ2M structure function was chosen for determining the theoretical jet shape.

8. Conclusion

Jets should narrow as the E_T of the jet increases since the transverse momentum of particles within the jet changes slowly with energy and the parallel momentum of particles within the jet changes approximately with energy, see fig. 1a. This measurement cannot be made at LO. The jet shape measurement is a first order measurement at NLO and large effects on the renormalization scale are expected. NLO theory qualitatively agrees with data, see fig. 1b. It correctly predicts the narrowing of jets as the E_T of the jets increase. Quantitatively, NLO does not describe the jet shape accurately. By changing the renormalization scale, it may be possible to correctly describe the jet shape at one particular E_T. Either higher orders must be taken into account or the effects of fragmentation are not negligible and must be included when calculating jet shapes.

References

1. *The Two-Jet Differential Cross Section at $O(\alpha_s^3)$ in Hadron Collisions.* W.T. Giele, E.W.N. Glover, D.A. Kosower, Fermilab-Pub-94/070-T
2. *The DØ Detector.* DØ collaboration, S. Abachi *et al*, Nucl. Inst. and Methods, **A338**,185 (1994)
3. *Measurement of Jet Shapes in $p\bar{p}$ Collisions at $\sqrt{s}$=1.8 TeV.* F. Abe *et al*, Phys Rev Lett, Vol 70, Number 6, 713 (1993)
4. *A study of differences between quark and gluon jets using vertex tagging of quark jets.* OPAL Collaboration, CERN-PPE/93-02, (1993)
5. Geant 3.14, R. Brun, *et al*, CERN

Fermi National Accelerator Laboratory

Use of a $K_\perp$ Jet Algorithm in $p\bar{p}$ Collisions at DØ

Katherine C. Frame

Michigan State University,
East Lansing, Michigan 48824-1116

Operated by Universities Research Association Inc. under Contract No. DE-AC02-76CHO3000 with the United States Department of Energy

USE OF A $K_\perp$ JET ALGORITHM IN $p\bar{p}$ COLLISIONS AT DØ

KATHERINE C. FRAME*
Physics-Astronomy Department, Michigan State University,
East Lansing,MI 48824-1116, USA

ABSTRACT

The determination of jet multiplicities with algorithms based on '$K_\perp$' type distance parameters at hadron colliders allows a more direct comparison to results from fixed target and e^+e^- experiments and has fewer theoretical ambiguities. We present the results of using such a jet definition to measure the fraction of events with 2, 3, and 4 jets at various momentum transfer (E_T) scales.

1. Introduction

A successive combination jet algorithm similar to those used in e^+e^- physics has been suggested by Ellis and Soper for hadron-hadron physics.[1] The algorithm provides an alternative to the presently used fixed cone algorithm and renders less ambiguity in counting jets. Each particle is assigned to one and only one jet and, therefore, the problem of splitting and merging of jets is avoided.

Because of its similarity to the $K_\perp$ (or Durham) algorithm[2] presently used at e^+e^- colliders, comparisons between hadron-hadron and e^+e^- physics becomes possible. Specifically, we are interested in using jet rates to measure α_S. At leading order, the fraction of events with 3 or more jets, R_3, can be written as*

$$R_3 = \frac{\sigma^{\geq 3jets}(LO)}{\sigma^{\geq 2jets}(LO)} \propto \alpha_S. \tag{1}$$

At the Tevatron, we can measure R_3 over a range of momentum transfer (E_T) scales from 50 to 500 GeV, and therefore, we will be able to probe the running of α_S.

2. The Algorithm

The algorithm suggested by Ellis and Soper clusters particles based on a function of $K_\perp$ type. But unlike the $K_\perp$-algorithm, it does not use a cutoff parameter, y_{cut}. Instead, particles are assigned to a jet if their separation in $\eta - \phi$ space is less than some value

$$R_{ij}{}^2 < D^2 \quad where \quad R_{ij}{}^2 = (\eta_i - \eta_j)^2 + (\phi_i - \phi_j)^2]. \tag{2}$$

The recombination procedure is as follows.

*Representing the DØ Collaboration.
*The NLO calculation for R_3 is expected within the next year.

1. For each pair of particles,i and j, we calculate the function

$$d_{ij} = minimum\left({E_{T,i}}^2, {E_{T,j}}^2\right) \frac{{R_{ij}}^2}{D^2} \tag{3}$$

where $D \approx 1$[†]. Then we define for each particle, i,

$$d_i = {E_{T,i}}^2. \tag{4}$$

2. The minimum d_{min} of all the d_i and d_{ij} is found.

3. If d_{min} is a d_{ij}, particles i and j are merged into a new, pseudo-particle k with

$$E_{T,k} = E_k \sin\theta_k, \quad \eta_k = -\ln\left(\tan\frac{\theta_k}{2}\right), \quad and \quad \phi_k = \arctan\frac{P_{x,k}}{P_{y,k}},$$
$$with\ four\ vector \quad {P_k}^\mu = {P_i}^\mu + {P_j}^\mu, \quad and \quad \theta_k = \arccos\frac{P_{z,k}}{|\vec{P_k}|}. \tag{5}$$

4. If d_{min} is a d_i (i.e. ${R_{ij}}^2 > D^2$ for all j), then the particle is deemed not "mergeable" and it is removed from the list of particles and placed in the list of jets.

5. Return to step 1. Repeat steps 1-5 until all particles have been merged into jets (i.e. ${R_{ij}}^2 > D^2$ for all ij). The result is a list of jets.

6. All jets with E_T below some fraction, f, of the hard scale are dropped [‡]. In this analysis, we used $E_{T,max}$ (leading jet E_T) to define the hard scale.

3. Analysis

The algorithm was performed on Herwig Monte Carlo data on partons (parton shower), particles (final state hadrons) and calorimeter cells (DØ detector simulation). Figures 1 and 2 show the fraction of events with 2, 3 and 4 jets as a function of f. The events were generated at 80 Gev E_T for the 2 to 2 process and analysed with $D = .7$. In figure 1, objects were merged as described above and give good agreement for $.2 < f < .4$. In figure 2, merging was done as prescribed by Ellis and Soper[1]:

$$E_{T,k} = E_{T,i} + E_{T,j}, \quad \eta_k = \frac{E_{T,i}\eta_i + E_{T,j}\eta_j}{E_{T,k}}, \quad and \quad \phi_k = \frac{E_{T,i}\phi_i + E_{T,j}\phi_j}{E_{T,k}}. \tag{6}$$

This method gives much less agreement. Thus, the method used in figure 1 was chosen.

Figure 3 shows the 2, 3 and 4 jet fractions for data taken from the first DØ data run (1992-1993) and Herwig Monte Carlo data at the parton shower level. Events are shown with $E_{T,max}$ between 88 and 100 Gev. The data appears to be in fairly good agreement with the Monte Carlo for $.2 < f < .35$, but diverge for larger f.

[†]It can be shown that for $D = 1$ and $R_{ij} << 1$, the function d_{ij} is approximately $K_{\perp,ij}$.

[‡]This was suggested by Mike Seymour and C-P. Yuan independently.

We are investigating alternative ways of defining the hard scale for each event . There is a worry that a bias toward 2 jet events is introduced by using $E_{T,max}$ to set the hard scale. We do see a decrease in R_3 for higher $E_{T,max}$ (figure 4), but at this point, we cannot confirm that it is due to the running of α_S. Studies of this are forthcoming and once confirmed, we will attempt to extract values of α_S for $100 < E_T < 500$ Gev.

References

1. S. D. Ellis, D. E. Soper, *Phys. Rev.* **D48** (1993) 3160.
2. S. Catani et al., *Phys.Lett.* **B285** (1992) 291.
3. S. Catani et al., preprint CERN-TH 6775/93.

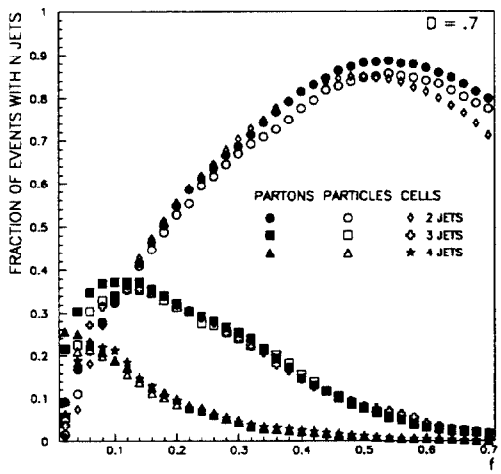

Fig. 1. Herwig data using addition of 4 vectors to merge objects.

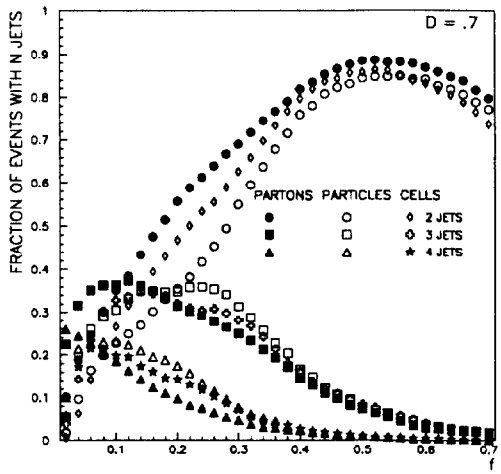

Fig. 2. Herwig data using an E_T weighted scheme to merge objects.

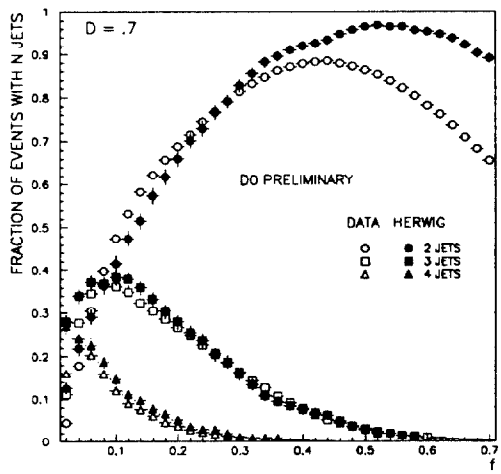

Fig. 3. DØ data and Herwig parton shower data with $88Gev < E_{T,max} < 100Gev$.

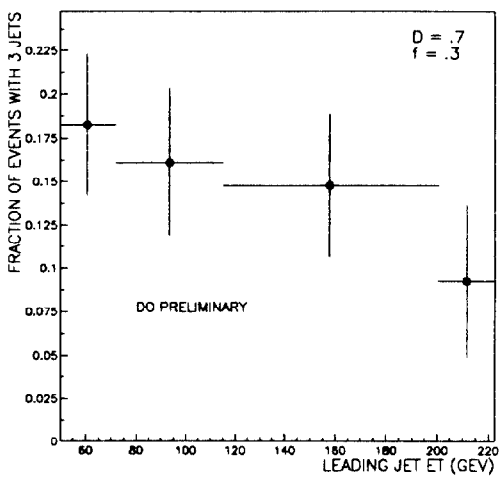

Fig. 4. The fraction of events with 3 jets vs. $E_{T,max}$.

Fermi National Accelerator Laboratory

Measurement of the Strong Coupling Constant (α_s) Using W+ Jets Processes in the DØ Detector

Jonathan Kotcher

Brookhaven National Laboratory,
Upton, Long Island, New York 11973

Operated by Universities Research Association Inc. under Contract No. DE-AC02-76CHO3000 with the United States Department of Energy

MEASUREMENT OF THE STRONG COUPLING CONSTANT (α_s) USING $W+$ JETS PROCESSES IN THE DØ DETECTOR

JONATHAN KOTCHER*
Brookhaven National Laboratory, Upton, Long Island, New York 11973 USA

ABSTRACT

We report a preliminary measurement of the strong coupling constant, α_s, extracted from 14.3 pb^{-1} of data taken at the Fermilab Tevatron collider with the DØ detector. We determine α_s from the ratio $R_\alpha = \sigma(W + 1\,\text{jet})/\sigma(W + 0\,\text{jets})$, where the W bosons are detected in the $W \to e\nu$ decay channel. The value obtained is $\alpha_s(M_W^2) = 0.126^{+0.018}_{-0.016}\,(\text{comb.})$.

1. Introduction

The fundamental parameter of Quantum Chromodynamics (QCD), the theory describing the strong interactions, is the strong coupling constant, α_s. The magnitude of the coupling strength, in that it describes our understanding of one of the fundamental forces in nature, and its dependence on the momentum transfer (Q^2) of the underlying process – i.e., quantitative experimental information on the "running" of α_s – are of basic experimental and theoretical interest.

We report below on the preliminary measurement of α_s at $Q^2 = M_W^2$ (where M_W is the mass of the W boson) in proton-antiproton collisions at a center of mass energy of 1.8 TeV. The measurement is based on 14.3 ± 1.7 pb^{-1} of data, which were collected with the DØ detector at the Fermilab Tevatron from August, 1992 to May, 1993. The large sample of W bosons produced at Tevatron energies ($\sigma \cdot \text{B}(W \to e\nu) \approx 2$ nb), in conjunction with improvements in our understanding of W production, have helped to motivate our measurement of this fundamental coupling in $W+$ jets processes at the Fermilab collider.

2. Triggering and Event Selection

The DØ detector is described in detail elsewhere.[1] Candidate $W \to e\nu$ events were required to satisfy certain calorimetric trigger requirements. The hardware trigger required 10 GeV of transverse energy in an electromagnetic tower of 0.2×0.2 in $\eta - \phi$ space and extended out to $|\eta| = 3.2$, which provided an acceptance of $> 99\%$ for electrons from W decay. The software trigger required an electromagnetic cluster of $E_T > 20$ GeV, and missing E_T ($\not\!\!E_T$) > 20 GeV. Loose shape and isolation cuts were also imposed on the electron. There were no jet requirements imposed at the trigger level.

*Representing the DØ collaboration

Offline, the cuts on the electron E_T and $\not\!\!E_T$ were increased to 25 GeV. A more stringent series of cuts were also applied to the electron to reduce background contamination. These included further isolation and shower shape cuts, a cut requiring more than 90% of the cluster energy to be deposited in the electromagnetic compartment of the calorimeter, and a requirement that there be a significant track match between a reconstructed track pointing from the drift chambers to the electron candidate cluster. In addition, there were cuts to select against noisy cells in the calorimeter, a requirement that the total scalar E_T in the event be consistent with a single $p\bar{p}$ interaction, and a cut requiring that there be one and only one electron with $E_T > 10$ GeV (to select against $Z \rightarrow ee$ decays). The total efficiency after geometric acceptance, trigger efficiency, and offline selection cuts was $33 \pm 2\%$, resulting in 9770 $W \rightarrow e\nu$ event candidates.

We selected jets offline using a fixed cone algorithm of radius $R_{jet} = 0.7$, where $R_{jet} = \sqrt{(\Delta\eta)^2 + (\Delta\phi)^2}$. Jet energies were corrected for calorimeter response, out-of-cone showering losses, pedestal noise, and the underlying event. We define the jet multiplicity as the number of jets with E_T greater than E_T^{min} after jet energy corrections, and have found that a value of $E_T^{min} = 25$ GeV provided sufficient statistics, while minimizing the experimental uncertainties.

3. Background Determination

We distinguish between two different background processes: "fake" backgrounds, and physics backgrounds. The "fake" backgrounds consist of QCD multi-jet events, wherein at least one jet, due to fluctuations in fragmentation and hadronization, passes all of the electron selection cuts, and imperfections in calorimetric coverage or response (cracks, non-linearities, etc.) result in significant $\not\!\!E_T$. These backgrounds have been determined directly from the data, and are found to be the dominant source of contamination. Physics backgrounds include $Z \rightarrow ee$, where one electron falls outside the detector acceptance, $Z \rightarrow \tau\tau$, with one τ decaying to an electron and two neutrinos and the other decaying hadronically, and mis-measured Drell-Yan background. These background rates have been determined by Monte Carlo simulation.

We find $8200.2 \pm 90.6(\text{stat})^{+52.3}_{-70.0}(\text{sys})$ $W + 0$ jet and $531.8 \pm 23.1(\text{stat})^{+54.4}_{-43.8}(\text{sys})$ $W + 1$ jet events after background subtraction, for $E_T^{min} = 25$ GeV. Details on the method of background determination may be found in Ref. 2.

4. Extraction of α_s

Measurements of α_s in the $W+$ jets channel in proton-antiproton collisions, using leading order theoretical calculations to extract a value for the coupling constant, have been reported from experiments at the CERN $p\bar{p}$ collider.[3] Recently, next-to-leading order (NLO) calculations have been incorporated into the Monte Carlo generator DYRAD,[4] in which the NLO $W + 0$ jets and $W + 1$ jet cross sections have been parametrized in the following manner:

$$\sigma(W + 0 \text{ jets}) = A_0 + \alpha_s A_1(E_T^{min}) \tag{1}$$

$$\sigma(W + 1 \text{ jet}) = \alpha_s B_0(E_T^{min}) + \alpha_s^2 B_1(E_T^{min}, R_{jet}). \tag{2}$$

Use of these NLO calculations reduces the theoretical uncertainty in the final measurement of α_s, as well as the dependence of the cross sections on the renormalization scale, μ_r.

The coefficients A_0, $A_1(E_T^{min})$, $B_0(E_T^{min})$, and $B_1(E_T^{min}, R_{jet})$ in Eqs. 1 and 2 are obtained from the Monte Carlo – it will be noticed that they contain no explicit dependence on α_s. They can, however, depend on both the minimum jet E_T cut (E_T^{min}) and the cone size used for jet finding, since the number of jets detected in the final state can depend on each of these parameters. The Monte Carlo was made to mimic features of the experimental analysis, such as acceptance, lepton isolation, and jet definition and resolution. This was done in order to keep to a minimum possible biases that may be induced by differences in systematics between experiment and theory.

To determine α_s, we obtain the ratio $R_\alpha = \sigma(W + 1 \text{ jet})/\sigma(W + 0 \text{ jets})$ from experiment. The four coefficients are provided by the Monte Carlo, allowing α_s to be computed directly from Eqs. 1 and 2 above. We choose the renormalization scale $\mu_r^2 = M_W^2$, and obtain the preliminary result:

$$\begin{aligned} \alpha_s(M_W^2) \;=\; & 0.126 \pm 0.005 \text{ (exp. stat.)} \pm 0.006 \text{ (MC stat.)} \pm \\ & 0.009 \text{ (theor. sys.)}^{+0.014}_{-0.011} \text{ (exp. sys.)}. \end{aligned} \tag{3}$$

The error is dominated by the experimental systematics – in this case, the jet energy scale uncertainty, which results in $\approx 10\%$ uncertainty in R_α. More data acquired during the current Tevatron running cycle will help us to reduce this uncertainty. The error attributed to theoretical systematics results from the differences between the structure functions used, while that due to Monte Carlo statistics is simply a reflection of the amount of Monte Carlo data generated, and can be made vanishingly small. It is clear from the above that we are no longer limited by experimental statistics in the present measurement.

Once the value of α_s is determined at some value of the renormalization scale, its magnitude at any other value of μ_r can be determined from the next-to-leading order QCD relation:

$$\alpha_s(\mu_r^2) = \alpha_s(M_W^2)[1 + \alpha_s(M_W^2)\, b_0\, ln(M_W^2/\mu_r^2)]. \tag{4}$$

(Here, b_0 is a constant that depends on the number of colors and the number of flavors.) Using this relation and the value for $\alpha_s(M_W^2)$ from Eq. 3, we obtain a value for α_s at $\mu_r^2 = M_Z^2$ (where M_Z = mass of the Z boson) of $\alpha_s(M_Z^2) = 0.123^{+0.017}_{-0.015}$(comb.), where the errors reflect a sum in quadrature of the values analogous to those in Eq. 3. This value is in good agreement with that from the LEP experiments at CERN of 0.123 ± 0.004.[5]

References

1. S. Abachi *et al.*, *Nucl. Instr. Meth.* **A338** (1994) 185.
2. Jaehoon Yu, Ph.D. Thesis, State University of New York at Stony Brook, Stony Brook, New York, 1993 (unpublished).
3. M. Lindgren *et al.*, *Phys. Rev.* **D45** (1992) 3038; J. Alitti *et al.*, *Phys. Lett.* **B263** (1991) 563.
4. W.T.Giele, E.W.N.Glover, and D.A. Kosower, *Nucl. Phys.* **B403** (1993) 633.
5. S. Banerjee, presented at the 10^{th} *DAE Symposium on High Energy Physics*, Bombay, India, (Dec. 1992), TIFR-EHEP-93-2 (Jan. 1993).

Fermi National Accelerator Laboratory

Measurement of the W/Z P_T Distributions at DØ

J. Zhi-Yu Jiang

State University of New York at Stony Brook,
Stony Brook, New York 11794

Operated by Universities Research Association Inc. under Contract No. DE-AC02-76CHO3000 with the United States Department of Energy

MEASUREMENT OF THE W/Z P_T DISTRIBUTIONS AT DØ

J. ZHI-YU JIANG*
Physics Department, State University of New York at Stony Brook
Stony Brook, NY 11794, U.S.A.

ABSTRACT

Based on 13.4 pb^{-1} of data collected by the DØ detector at Fermilab during the 1992-1993 $p\bar{p}$ collider run, we have measured the transverse momentum spectra of W/Z bosons observed in the electron decay channel. Preliminary results are compared with theoretical predictions.

1. Introduction

At $\bar{p}p$ colliders, W and Z bosons may have p_T due to the production of gluons and quarks (from initial state radiation) along with the gauge bosons. QCD predictions for the inclusive p_T spectra of W and Z are available for all values of p_T.[1] Parameterization of the nonperturbative function at low p_T region has been optimized recently.[2]

In the electronic decay mode, i.e. $W \rightarrow e\nu + X$ and $Z \rightarrow ee + X$, p_T^Z can be reconstructed by the transverse momenta of decay electrons with very good resolution, whereas p_T^W can only be reconstructed by the recoil p_T with large uncertainty. The p_T^Z measurement is limited by statistics at large p_T but has more sensitivity at low p_T for testing resummation and nonperturbative QCD. On the other hand, the p_T^W measurement is dominated by underlying events at low p_T but has better statistical precision and smaller relative error at high p_T for testing perturbative QCD.

2. Data Sample

2.1. Triggering and Electron ID

The data for this analysis were accumulated under a single electron trigger with an E_T threshold of 20 GeV.

Electron candidates are identified in the offline reconstruction by forming nearest-neighbor clusters of EM calorimeter readout towers. The offline selection criteria for electron identification are: Cluster Electromagnetic Energy Fraction: > 90%; Cluster Shape $\chi^2 < 100$ for the Central Calorimeter, $\chi^2 < 200$ for the End Calorimeter; Cluster Isolation < 0.15; Cluster–Track Matching Significance< 10. Details of the DØ electron identification have been described previously.[3]

2.2. W/Z Selection

The W candidate sample is selected by requiring the presence of one electron and large $\not\!\!E_T$ with the electron $E_T > 25$ GeV and the $\not\!\!E_T > 25$ GeV.

*Representing the DØ Collaboration.

The Z candidate sample is selected by requiring the presence of two electrons each with $E_T > 25$ GeV and the di-electron invariant mass between 75 GeV and 105 GeV.

Electrons are required to be in the well-measured regions of the detector, which are defined as $|\eta| < 1.1$ and $1.5 < |\eta| < 2.5$ (where the pseudorapidity $\eta \equiv -\ln[\tan(\theta/2)]$, and θ is the polar angle with respect to the proton-beam direction). Central electrons within $\pm$ 0.01 radians of the azimuthal boundaries between calorimeter modules, which occur every 0.2 radians, are also rejected. The absolute energy scale of the EM calorimeters is set by scaling the invariant mass peak to the LEP value for the Z mass[4] before the kinematic cuts.

2.3. Background Estimation

In the W sample, there are estimated 3.3% background from QCD multijet events, 1.9% from $W \rightarrow \tau\nu$ events, and 0.7% from $Z \rightarrow ee$ events. In the Z sample, there are estimated 3.5% background from QCD multijet events, 1.3% from Drell-Yan continuum events, and negligible $Z \rightarrow \tau\tau \rightarrow ee$ contribution. The p_T distributions of the background events are similar to those of the signal events.[5]

3. Monte Carlo Simulation

The differential cross sections ($\frac{d\sigma}{dp_T dy}$, y is rapidity) for W/Z production from Arnold-Kauffman and Ladinsky-Yuan calculations are used as inputs to a fast W/Z Monte Carlo program. All detector effects are included and the W/Z p_T distributions reconstructed. Detailed comparisons on many features between the Monte Carlo simulation and data are performed to establish the model.[5] The comparisons on rapidity and the Feynman X distributions of Z show good agreement. We then compare the smeared theoretical p_T distributions with data.

4. Results and Conclusion

The average measurement error on p_T^W is about 5.0 GeV dominated by underlying events E_T. Monte Carlo simulation indicates that the average measurement error on p_T^Z is 1.6 GeV, mainly due to electron energy resolution. Figure 1 and Fig. 2 show the results for p_T^W and p_T^Z respectively. The preliminary results show good agreement for the large p_T region. Theoretical models at small p_T region can be further constrained with our data.

References

1. P. B. Arnold and R. P. Kauffman, *Nucl. Phys.* **B349**(1991)381; P. B. Arnold and M. H. Reno, *Nucl. Phys.* **B319** (1989)37; J. Collins, D. Soper and G. Sterman, *Nucl. Phys.* **B250** (1985) 199.
2. G. A. Ladinsky and C.-P. Yuan, *MSUHEP-93/20* (1993)
3. M. Narain, *Proceedings of the DPF'92 meeting at Fermilab*, 1678.
4. The LEP collaborations: ALEPH, DELPHI, L3 and OPAL. Phys. Lett. **B276**, 247 (1992).
5. J. Z-Y. Jiang, *Ph.D. Thesis*, State University of New York at Stony Brook (1994).

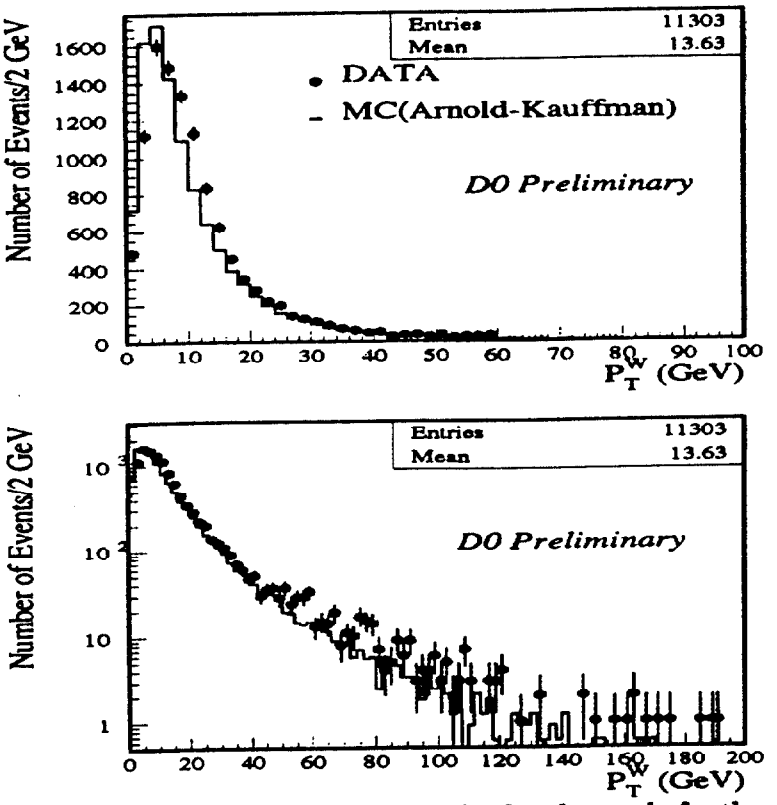

Fig. 1. The p_T^W measurement. The bottom plot has log scale for the vertical axis.

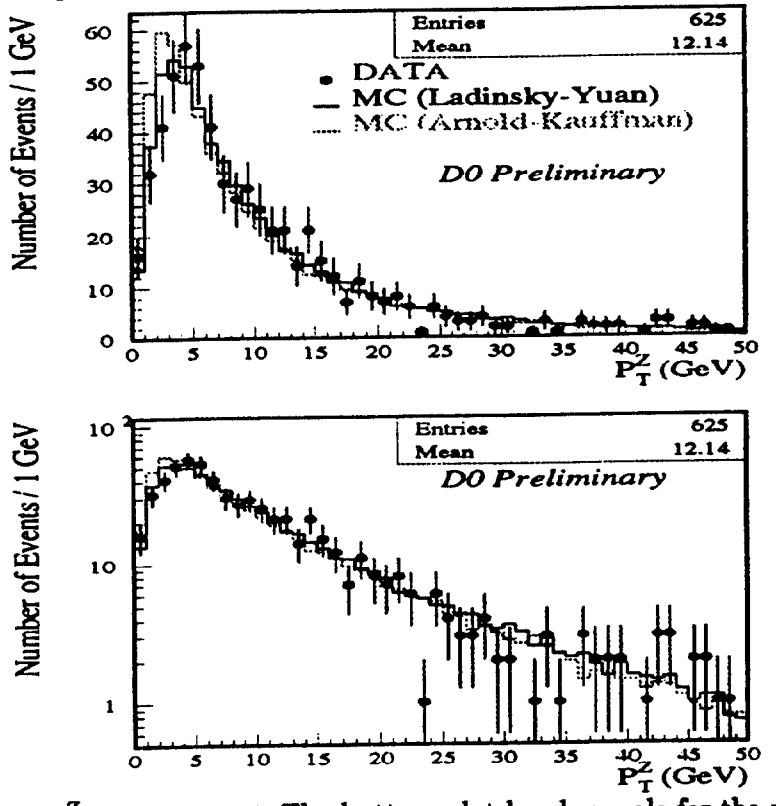

Fig. 2. The p_T^Z measurement. The bottom plot has log scale for the vertical axis.

Fermi National Accelerator Laboratory

Jet Production at Large Rapidity Intervals

T. Heuring

Florida State University,
Tallahassee, Florida 32306

Operated by Universities Research Association Inc. under Contract No. DE-AC02-76CHO3000 with the United States Department of Energy

JET PRODUCTION AT LARGE RAPIDITY INTERVALS

T.Heuring*
Department of Physics, Florida State University,
Tallahassee, FL 32306 USA

ABSTRACT

During the 1992–93 collider run of the Fermilab Tevatron the DØ experiment accumulated a large sample of events with jets in the final state. Since DØ has the ability to trigger on jets out to a pseudorapidity of 3.2, we were able to collect events containing jets with large rapidity intervals. Such events may not be well described by LO or NLO QCD perturbative calculations due to the increased importance of additional gluon radiation which tends to decorrelate the leading jets in the event. These contributions can be included by using BFKL theory to resum the leading powers of the rapidity interval to all orders in α_s. We present the first experimental measurement of jet-jet ϕ correlations as a function of the rapidity interval of the η ordered jets. We compare these results to JETRAD, HERWIG and BFKL resummation predictions.

1. Introduction

Theoretical QCD calculations of jet final states resulting from $\bar{p}p$ collisions have historically been dominated by fixed order expressions. Leading order (LO) and next-to-leading order (NLO) calculations[1,2] have so far provided an adequate description of the measured cross sections.[3] As new regions of phase space are explored limitations of this approach may be encountered. If there is more than one scale present in the process the perturbative calculation will contain logarithms of the ratios of these quantities; these logarithms may become large. An appropriate choice of the renormalization scale can absorb one of these scales into the parton distribution function, but the others will remain in the perturbative expansion. Such scales arise when low E_T jets with large rapidity intervals are produced at the Tevatron.

DelDuca and Schmidt,[4] and independently Stirling,[5] have developed techniques based on the theory of Balitsky-Fadin-Kuraev-Lipatov[6] (BFKL) to resum these large logarithms. BFKL theory resums to all orders in α_s soft gluon emissions that arise in these cases. Their calculation leads to a term e^y appearing in the partonic cross section where y is the rapidity interval between the two jets most separated in rapidity. This indicates that this emission should increase exponentially as a function of y. Such emissions would tend to decorrelate the two leading jets. In the case of fixed order

*Representing the D0 Collaboration.

calculations little or no decorrelation would be seen. In LO, the jets are always correlated but in NLO, the presence of one additional parton will induce some decorrelation, weakly dependent on y.

We have investigated this decorrelation by analyzing azimuthal angle distributions between jets in events with large rapidity intervals in collider data and compared them to predictions from BFKL resummation, HERWIG[7] and JETRAD[8] (a NLO Monte Carlo) . We calculated $\pi - \Delta\phi$ where $\Delta\phi$ is the difference in azimuth between the jets with the largest rapidity interval $\Delta\eta = \eta_1 - \eta_2$. We plotted $\xi = < \cos(\pi - \Delta\phi) >$ as a function of $\Delta\eta$. Complete correlation would correspond to ξ = constant for all $\Delta\eta$; decorrelation would be indicated by a deviation from the constant. Unfortunately, calculations are not currently available using the cuts we applied to the data, forcing us to compare HERWIG and JETRAD to each separately. Efforts are underway to produce calculations compatible with our data.

2. Detector and Event Selection

The DØ detector was used for this study. As it is described in detail elsewhere,[9] only the portions relevant to this analysis will be described here. DØ has a uranium–liquid argon sampling calorimeter covering the pseudorapidity region $|\eta| < 4.0$ and 2π in ϕ. It has fine longitudinal and transverse segmentation providing good jet energy and position resolution.

The trigger consists of three levels. The first (L0) requires hits in beam-beam scintillation counters signalling the presence of an inelastic collision. The second level (L1) looks for localized energy deposits in 0.2×0.2 ($\Delta\eta \times \Delta\phi$) towers in the calorimeter. The third level (L2) implements a cone based jet-finding algorithm ($R = 0.7$) using calorimeter cell information. Jets were triggered on out to $\eta = 3.2$. For this analysis, one tower above 7 GeV at L1 and 1 jet above 30 GeV at L2 were required.

Jet energy scale corrections were applied offline and spurious jets removed before a minimum E_T cut of 20 GeV was applied. Of the remaining jets, the one most forward will be referred to as jet 1 and the one furthest away in rapidity from jet 1 will be referred to as jet 2. One of these two 'tagging' jets was required to be above 50 GeV to remove any trigger bias.

3. Results

Currently the BFKL calculation is available using symmetric cuts where both tagging jets were required to be above the same threshold. The comparison between HERWIG, JETRAD and the BFKL resummation calculation are shown in Figure 1 for $E_{t1,2} > 30$ GeV. Here we see that the resummation theory predicts a much stronger decorrelation effect than seen in HERWIG or JETRAD; these show reasonable agreement possibly due to the radiation suppressing effects of the symmetric cuts. Experimental data should be able to distinguish between these predictions.

In Figure 2 the comparison between HERWIG, JETRAD and collider data for the cuts described in Section 2 are shown. Here we see that there is good agreement between HERWIG and the data. In contrast, there is a difference in the shape of the distribution for JETRAD which predicts too little decorrelation for these selection criteria.

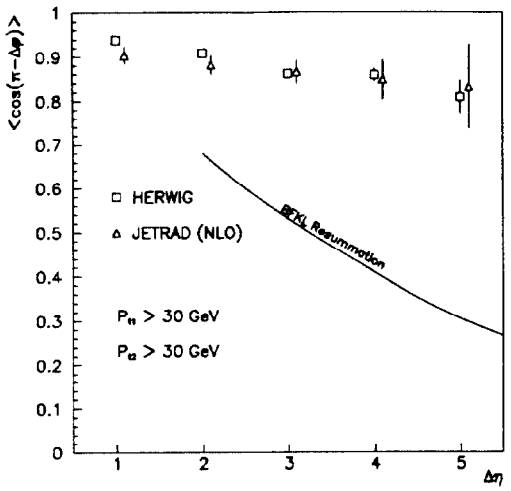

Fig. 1. $< cos(\pi - \Delta\phi) >$ v. $\Delta\eta$ for symmetric 30/30 GeV E_t cuts.

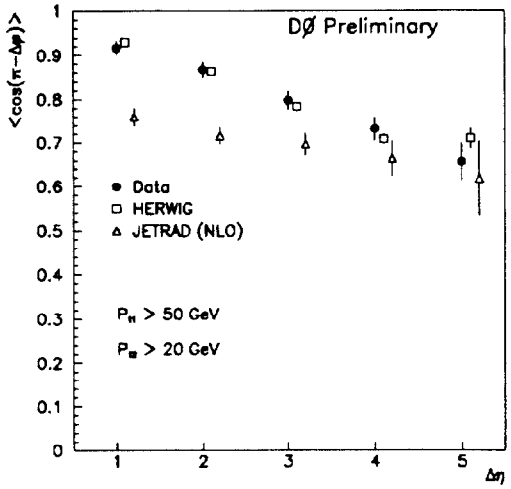

Fig. 2. $< cos(\pi - \Delta\phi) >$ v. $\Delta\eta$ for asymmetric 50/20 GeV E_t cuts.

4. Conclusions

We have examined jet-jet correlations in jets produced with large rapidity intervals using the DØ detector at the Tevatron. These events show a decorrelation in azimuth between the extreme η jets which increases with increasing $\Delta\eta$. These effects are described well by HERWIG but NLO calculations show a weaker trend. Theoretical predictions based on BFKL theory are not directly comparable at this time, but comparisons between this calculation and HERWIG and NLO predictions with similar event selection criteria show a much stronger decorrelation effect for the resummation theory than HERWIG or NLO.

References

1. S.D. Ellis, Z. Kunszt and D.E. Soper, Phys. Rev. D **40**, 2188 (1989); Phys. Rev. Lett. **64**, 2121 (1990).
2. W.T. Giele, E.W.N. Glover and D.A. Kosower, Fermilab preprint FERMILAB-Pub-94/070-T (1994).
3. D.Elvira, "Inclusive Jet Cross Sections at DØ", these proceedings;
   F. Abe et al., CDF Collab., Fermilab preprint FERMILAB-Conf-93/201-E (1993).
4. V. Del Duca and C.R. Schmidt, Phys. Rev. D **49**, 4510 (1994); preprint DESY 94-114 (1994).
5. W.J. Stirling, preprint DTP/94/04 (1994).
6. L.N. Lipatov, Yad. Fiz. **23**, 642 (1976) [Sov. J. Nucl. Phys. **23**, 338 (1976)];
   E.A. Kuraev, L.N. Lipatov and V.S. Fadin, Zh. Eksp. Teor. Fiz. **71**, 840 (1976) [Sov. Phys. JETP **44**, 443 (1976)]; **72**, 377 (1977) [**45**, 199 (1977)];
   Ya.Ya. Balitsky and L.N. Lipatov, Yad. Fiz. **28** 1597 (1978) [Sov. J. Nucl. Phys. **28**, 822 (1978)].
7. G.Marchesini and B.R.Webber, Nucl. Phys. **B310**, 461 (1988).
8. W.T. Giele, E.W.N. Glover and D.A. Kosower, Nucl. Phys. **B403**, 633 (1993).
9. S. Abachi *et al.*, Nucl. Instr. & Meth. **A338**, 185 (1994).

Fermi National Accelerator Laboratory

Rapidity Gaps Between Jets at DØ

Brent J. May

University of Arizona
Tucson, Arizona 85721

Operated by Universities Research Association Inc. under Contract No. DE-AC02-76CHO3000 with the United States Department of Energy

AZPH-EXP/94-02
D0Note 2243

RAPIDITY GAPS BETWEEN JETS AT DØ

BRENT J. MAY*
Department of Physics, University of Arizona
Tucson, AZ 85721

ABSTRACT

Results are presented from a search for events with a rapidity gap between high transverse momentum jets produced in the Fermilab Tevatron $p\bar{p}$ collider at $\sqrt{s} = 1.8\,\text{TeV}$. The DØ detector is used to tag particles between the two highest transverse energy jets with $E_T > 30\,\text{GeV}$. A significant excess of events is observed at low tagged particle multiplicity which is qualitatively consistent with a color-singlet exchange process.

Rapidity gaps, namely regions of rapidity containing no final-state particles, are expected to occur between jets when a color-singlet is exchanged between the interacting hard partons.[1] The exchange of a photon,[2] $W^{\pm}$, Z^0 or hard QCD Pomeron[3,4] is expected to give such an event topology. Although the cross section for electroweak gauge boson exchange is small, the cross section for two-gluon Pomeron exchange is believed to be significant,[3,5] and roughly 10% of jet events may be due to Pomeron exchange.[3] Typical color-octet jet events (single gluon or quark exchange) have particles between jets, but rapidity gaps can arise from fluctuations in the particle multiplicity, which is expected to have a negative binomial or similar distribution.[6]

Rapidity gaps will not be observed in the final state, however, if spectator interactions produce particles between the jets. Approximately 10-30% of rapidity gap events are expected to survive spectator interactions.[3,7] Thus roughly 1-3% of jet events are expected to have an observable rapidity gap between the jets from Pomeron exchange.

Although it is not possible to distinguish color-singlet rapidity gaps from those that occur in color-octet exchange on an event-by-event basis, differences in the expected particle multiplicity distributions can be used to search for a color-singlet signal. This signal is expected to appear as an excess of events at low particle multiplicity compared to a negative binomial-like distribution.

The data sample used in this analysis is derived from a special high-$\Delta\eta_c$ trigger[8] implemented to obtain events with large pseudorapidity separation ($\Delta\eta_c = |\eta_1 - \eta_2| - 2R$) between the cone edges ($R = \sqrt{\Delta\eta^2 + \Delta\phi^2} = 0.7$) of the two highest E_T jets. In the offline analysis, events are required to have at least two jets, each with $E_T > 30\,\text{GeV}$ and $|\eta| > 2$. Events with more than one interaction in a proton-antiproton crossing are removed since they include a source of particles not associated with the triggering interaction. The calorimeter[9] is used to measure the multiplicity distribution of tagged particles between the two highest E_T jets. Particles are tagged in the electromagnetic section of the calorimeter by requiring $E_T > 200\,\text{MeV}$ in a calorimeter tower.[8]

*Representing the DØ Collaboration

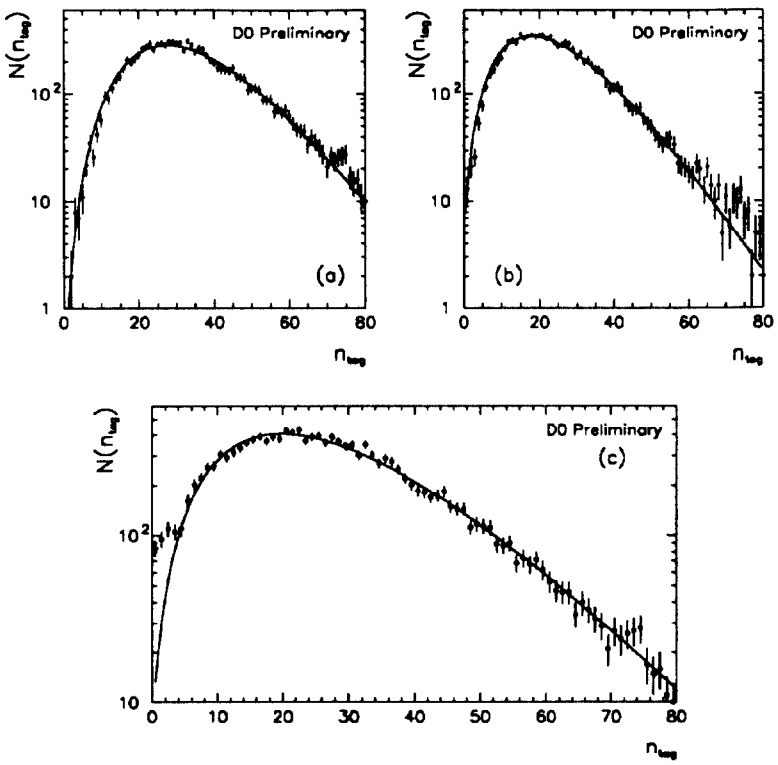

Fig. 1. The tagged particle multiplicity distributions obtained from color-octet events (a,b) and the inclusive event sample (c) for $\Delta\eta_c > 3$. Negative binomial fits to the data (solid lines) are also shown.

Although the color-octet particle multiplicity between jets is expected to have a negative binomial-like distribution, it is important to show that detector effects do not cause a significant deviation from the expected distribution, especially at low multiplicity. The Monte Carlo PYTHIA has been shown to be consistent with negative binomial particle multiplicity distribution between jets for events generated with conditions similar to the high-$\Delta\eta_c$ trigger.[10] Simulation of the DØ geometric acceptance and particle tagging efficiency gives a multiplicity distribution which is also consistent with a negative binomial distribution. No deviation is observed at low multiplicity, indicating that detector effects do not generate an artificial excess.

An enriched color-octet subsample of the data was also studied. This sample was obtained by requiring a jet (E_T >8 GeV) to be in the $\Delta\eta_c$ region between the two leading jets. Figure 1(a) shows the tagged particle multiplicity distribution between the two highest E_T jets for $\Delta\eta_c > 3$. Figure 1(b) shows the multiplicity distribution between the jets after excluding the multiplicity of tagged particles within a cone of $R = 0.7$ of the jet in the $\Delta\eta_c$ region. Both distributions are consistent with a negative binomial distribution.

The inclusive tagged particle multiplicity distribution for events with $\Delta\eta_c > 3$ is shown in Fig. 1(c). A very significant (41σ) excess is observed at small particle multiplicity compared to a negative binomial fit. The starting bin of the fit has been

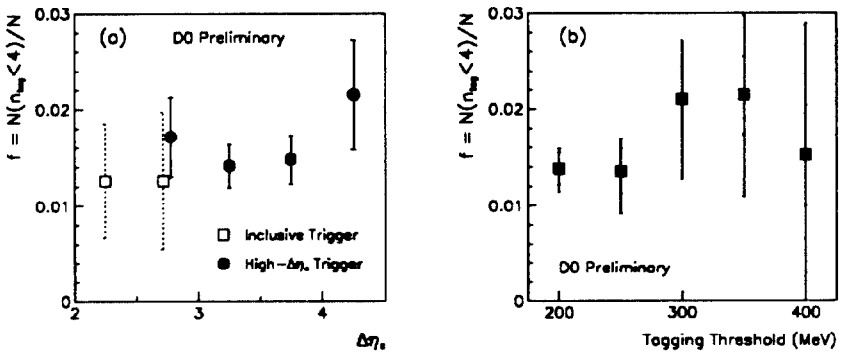

Fig. 2. The fractional excess $f = N(n_{tag} < 4)/N$ above a negative binomial fit to the tagged particle multiplicity distribution as a function of $\Delta\eta_c$ (a) and tagging threshold (b).

chosen to minimize the resulting χ^2. Fitting the entire distribution gives a χ^2/df of 2.1 while starting the fit at $n_{tag} = 4$ gives a much improved χ^2/df of 0.9. Fitting at higher n_{tag} does not improve the quality of the fit.

The excess above the fit has been determined by subtracting the negative binomial fit from the data for $n_{tag} < 4$. A preliminary fractional excess of $f = N(n_{tag} < 4)/N = (1.4 \pm 0.2^{(stat)} \pm 0.2^{(fit)}) \times 10^{-2}$ is obtained, where the systematic error has been obtained by varying the starting point of the fit in the range $0 \leq n_{tag} \leq 10$. The observed excess is relatively constant with $\Delta\eta_c$ as shown in Fig. 2(a) and not strongly dependent on the calorimeter tagging threshold (Fig. 2(b)) although the systematic error of fitting becomes larger with higher thresholds.

DØ has measured the tagged particle multiplicity distribution between jets. A significant excess of events is observed at low tagged particle multiplicity compared to a negative binomial distribution. This excess is consistent with expectations for a color-singlet exchange process, possibly indicating observation of a strongly interacting color-singlet.

References

1. Y. Dokshitzer, V. Khoze and S. Troyan, *Proc. of the 6th Int. Conf. on Phys. in Collisions* (1986), ed. M. Derrick (World Scientific, Singapore, 1987).
2. R. S. Fletcher and T. Stelzer, Phys. Rev. D**48**, 5162 (1993).
3. J. D. Bjorken, Phys. Rev. D**47**, 101 (1992).
4. H. Chehime and D. Zeppenfeld, preprint MAD/PH/814 (1994).
5. V. Del Duca and W. K. Tang, preprint SLAC-PUB-6310 (1993).
6. I. Dremin, submitted to Physics Uspekhi, FIAN TD-6, (1994) and references therein.
7. E. Gotsman, E. M. Levin and U. Maor, Phys. Lett. B**309**, 199 (1993).
8. S. Abachi *et al.*(DØ Collaboration), Phys. Rev. Lett. 72, 2332 (1994).
9. S. Abachi *et al.* (DØ Collaboration), Nucl. Instrum. and Meth. A**338**, 185 (1994).
10. R. Fletcher, private communication.

Fermi National Accelerator Laboratory

Probing Color Coherency Using High pT W Events at the Tevatron

G.E. Forden

University of Arizona
Tucson, Arizona 85721

Operated by Universities Research Association Inc. under Contract No. DE-AC02-76CHO3000 with the United States Department of Energy

Probing Color Coherency Using High pT W Events at the TEVATRON

G.E. Forden*
Department of Physics, University Arizona,
Tucson AZ

ABSTRACT

DØ has used $W \rightarrow e\nu$ events associated with a high pT jet to probe for the effects of extended source color dipole radiation in W-jet rapidity correlations. We have also studied the low energy flow in these events and shown an enhancement between the jet and the beam directions, indicating the effects of color coherency.

Charged W bosons are produced in $p\bar{p}$ events predominantly by two processes, the annihilation process and a diagram similar to Compton scattering. In both processes a color charge is removed from each incident hadron leaving an extended colored object, the proton remnants. This situation, far from being too "dirty" to provide useful information, is in fact a brilliant place to study radiative corrections. DØ has used events where a W, observed in the $e\nu$ channel, is produced in conjunction with a jet to study both the low energy flow referred[1] to as the "string drag effect" and a new measurement designed to probe the possibility that the primary jet is radiated by a spatially extended colored object. This later effect is expected to manifest itself as a reduction of the phase space available to the jet in the large pseudo-rapidity (η) regions for forward W's. We searched for this effect by studying the W-jet rapidity correlations.

Both analyses use similar W candidate selection criteria which are essentially those out lined in Reference 2. In addition both studies require the presence of a good,[3] primary jet with some minimum pT. It is necessary to reconstruct the W's rapidity for both these studies. This is done by constraining the W candidate to have the world average mass, 80.22 GeV. This results, in general, in two possible solutions for the W's longitudinal momentum. We can not use the electron charge to help resolve this ambiguity since DØ does not have a central magnetic field. Instead, we always choose the solution with the lower $|P_z(W)|$. Monte Carlo studies have indicated that this gives the correct solution the most often, given our knowledge of the event. It should be pointed out that W's reconstructed with large rapidities by this method have a large ($> 80\%$) chance of being correctly reconstructed. This algorithm systematically moves W's which were produced with large rapidities (but with a correspondingly smaller cross section) to the central region, which minimizes the effect of this systematic shift. This same algorithm is also used on Monte Carlo events in any comparisons performed.

The lowest order diagrams for the production of a high pT W all have an internal quark line whose virtuality is directly related to the W-Jet system invariant mass.

*Representing the DØ Collaboration

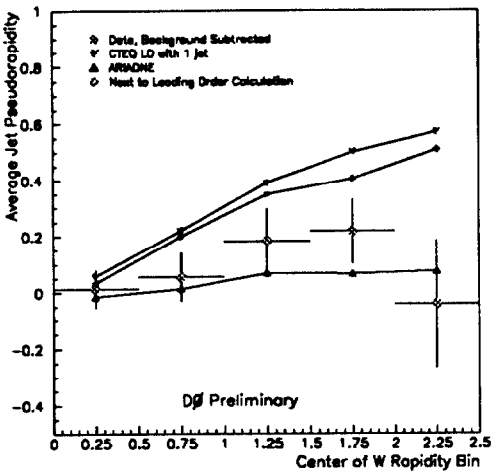

Fig. 1. The average jet rapidity of the primary jet as a function of reconstructed W rapidity. The LO, NLO and ARIADNE Monte Carlo predictions are also shown.

This mass tends to be minimized by the internal quark propagator. This can be accomplished when the W and jet have the same rapidity, but of course are opposite in ϕ. This behavior can be modified by various processes. The parton density functions might systematically inhibit various kinematicly allowed topologies. Color coherence effects producing radiated gluons preferentially between the primary jet and the beam remnants could systematically recoil the primary jet towards lower rapidities. Another possibility, as mentioned above, is that interference effects involving all the incident hadrons[4] constituents could restrict the primary jet to central rapidities.

We have studied the W-jet rapidity correlation for events where there is a jet produced with $pT > 16GeV$ and compared it to various Monte Carlos reflecting lowest order,[5] next to leading order[6] and extended color dipole[7] predictions. The average jet rapidity as a function of the W rapidity is shown in Figure 1 together with the predictions for the various Monte Carlos. It is clear that none of the Monte Carlos do a particularly good job of describing the data. However, by performing a χ^2 analysis on the actual jet rapidity distributions for those events with W rapidities greater than 1.0 we can exclude the leading order and the next to leading order at the 95% confidence level while there is an 18% chance that the discrepancies between ARIADNE, the color dipole model, and the data are due to statistical fluctuations alone.

We select those $W \rightarrow e\nu$ events which have a central jet with pT > 10 GeV and a reconstructed central W to compare the energy flow in an annulus around the jet and the corresponding annulus around the W. Both production mechanisms, the annihilation and the Compton scattering, produce at least one color string between the jet and a beam remnant (the annihilation process produces two, one to each remnant) and none to the color neutral W. The string drag effect should produce an increased energy flow on the line between the jet and either beam while this increase should not be present on the W side of the event. The inner radius of each annulus is $\Delta R = 0.7$ which corresponds to the standard DØ jet cone while the outer radius is $\Delta R = 1.5$.

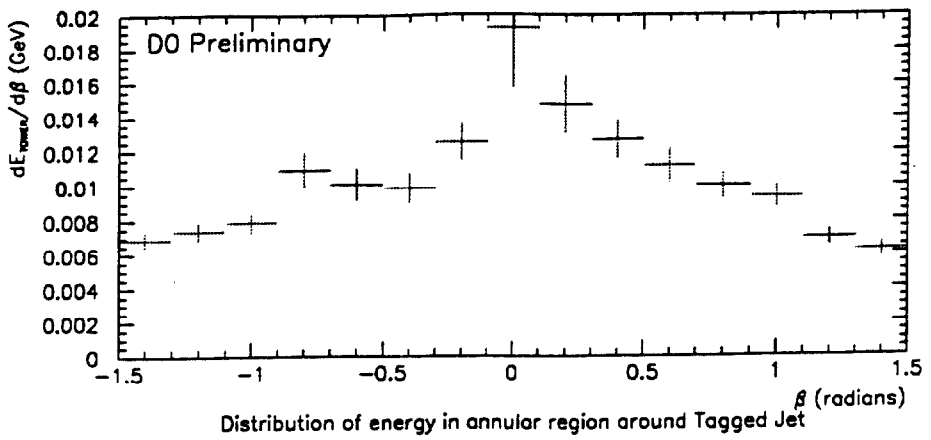

Fig. 2. The energy flow around the jet, $dE/d\beta$, as a function of the angle β which is zero in the direction of the beam.

Polar coordinates centered on these cones are used to determine the energy flow with respect to the closest beam direction. We define a polar angle β which is zero in the direction of the beam. The energy flow $dE/d\beta$ is then the radial integral of this energy as a function of β. The resulting measurement of the energy around the jet is shown in Figure 2. The corresponding energy around the W does not show this enhancement at $\beta = 0$, the direction toward the beam. This is in qualitative agreement with analytic calculations by Dokshitzer et al.[8]

DØ has measured the rapidity correlation between high pT W's and the primary jets. We find that the jet stays central almost independent of the W's rapidity. This is in conflict with the leading order (LO) and next to leading order (NLO) QCD expectations which predict that the jet should follow the W's rapidity. The Monte Carlo ARIADNE, which is based on radiation patterns being determined by extended color dipoles, qualitatively predicts this and can not be ruled out. We have also shown that the low energy flow in high pT W events is in qualitative agreement with coherent radiation pattern predictions.

References

1. Yu. L. Dokshitzer *et al. Basics of Perturbative QCD* Editions Frontieres, Gif-sur-Yvette Cedex - France, 1991
2. N. Graf "Production of W and Z bosons at DØ " To appear in the 9^{th} Topical Workshop on Proton- Anti-proton Collider Physics Proceedings, Tsukuba, Japan 18-22 Oct. 1993.
3. H. Weerts "Studies of Jet Production with the DØ Detector" To appear in the 9^{th} Topical Workshop on Proton-Anti-proton Collider Physics Proceedings, Tsukuba, Japan 18-22 Oct. 1993.
4. B. Andersson, Private Communication.
5. I. Hinchliffe LBL-34372, Submitted to Workshop on Physics at Current Accelerators and the Supercollider, Argonne, IL, 2-5 Jun 1993
6. W.T. Giele, E.W.N. Glover, D. A. Kosower Phys. Lett. B**309** 205 (1993)
7. L. Lönnblad, Comp. Phys. Comm. **71** 15 (1992). We have used ARIADNE version 4.05P02 in this analysis.
8. Yu.L. Dokshitser *et al.* Nucl.Phys.B**387**, 675-714 (1992)